Review

New Phytologist

Tansley review

Energy costs of salt tolerance in crop plants

Author for correspondence:
Stephen D. Tyerman
Tel: +61 831 36663
Email: steve.tyerman@adelaide.edu.au

Received: *21 December 2018*
Accepted: *25 March 2019*

Rana Munns[1,2]*, David A. Day[3]*, Wieland Fricke[4]*, Michelle Watt[5]*, Borjana Arsova[5], Bronwyn J. Barkla[6], Jayakumar Bose[7], Caitlin S. Byrt[7,8], Zhong-Hua Chen[9], Kylie J. Foster[10], Matthew Gilliham[7], Sam W. Henderson[11], Colin L. D. Jenkins[3], Herbert J. Kronzucker[12], Stanley J. Miklavcic[10], Darren Plett[12], Stuart J. Roy[13], Sergey Shabala[14,15], Megan C. Shelden[7], Kathleen L. Soole[3], Nicolas L. Taylor[16], Mark Tester[17], Stefanie Wege[7], Lars H. Wegner[18] and Stephen D. Tyerman[7]

[1]Australian Research Council (ARC) Centre of Excellence in Plant Energy Biology, and School of Agriculture and Environment, The University of Western Australia, Crawley, WA 6009, Australia; [2]CSIRO Agriculture and Food, Canberra, ACT 2601, Australia; [3]College of Science and Engineering, Flinders University, GPO Box 2100, Adelaide, South Australia 5001, Australia; [4]School of Biology and Environmental Sciences, University College Dublin (UCD), Dublin, 4, Ireland; [5]Plant Sciences, Institute of Bio and Geosciences, Forschungszentrum Juelich,Helmholtz Association, 52425, Juelich, Germany; [6]Southern Cross Plant Science, Southern Cross University, Lismore, NSW 2481, Australia; [7]Australian Research Council (ARC) Centre of Excellence in Plant Energy Biology, School of Agriculture, Food and Wine, University of Adelaide, Glen Osmond, SA5064, Australia; [8]Research School of Biology, Australian National University, Canberra, ACT 2600, Australia; [9]School of Science and Health, Western Sydney University, Penrith, NSW 2751, Australia; [10]Phenomics and Bioinformatics Research Centre, School of Information Technology and Mathematical Sciences, University of South Australia, Mawson Lakes, SA 5095, Australia; [11]Commonwealth Scientific and Industrial Research Organisation, Agriculture and Food, Urrbrae, SA 5064, Australia; [12]School of Agriculture and Food, Faculty of Veterinary and Agricultural Sciences, The University of Melbourne, Melbourne, VIC 3010, Australia; [13]Australian Research Council (ARC) Industrial Transformation Research Hub for Wheat in a Hot and Dry Climate, School of Agriculture, Food and Wine, University of Adelaide, Urrbrae, SA 5064, Australia; [14]Tasmanian Institute for Agriculture, University of Tasmania, Private Bag 54, Hobart, Tas. 7001, Australia; [15]International Centre for Environmental Membrane Biology, Foshan University, Foshan 528000, China; [16]Australian Research Council (ARC) Centre of Excellence in Plant Energy Biology, School of Molecular Sciences and Institute of Agriculture, The University of Western Australia, Crawley, WA 6009, Australia; [17]Biological and Environmental Sciences & Engineering Division (BESE), King Abdullah University of Science and Technology (KAUST), Thuwal 23955-6900, Saudi Arabia; [18]Karlsruhe Institute of Technology, Institute for Pulsed Power and Microwave Technology (IHM), D-76344, Eggenstein-Leopoldshafen, Germany

Contents

	Summary	1073
I.	Introduction	1073
II.	Tissue respiration and energy supply	1073
III.	Water and ion transport	1077
IV.	Root anatomy and transport pathways	1083
V.	Where to from here?	1085
	Acknowledgements	1086
	References	1086

*These authors contributed equally to this work.

New Phytologist (2020) **225:** 1072–1090
doi: 10.1111/nph.15864

Key words: barley and wheat, energy costs, membrane transport, photosynthesis, respiration, root anatomy, salt tolerance, sodium and chloride transport.

Summary

Agriculture is expanding into regions that are affected by salinity. This review considers the energetic costs of salinity tolerance in crop plants and provides a framework for a quantitative assessment of costs. Different sources of energy, and modifications of root system architecture that would maximize water vs ion uptake are addressed. Energy requirements for transport of salt (NaCl) to leaf vacuoles for osmotic adjustment could be small if there are no substantial leaks back across plasma membrane and tonoplast in root and leaf. The coupling ratio of the H^+-ATPase also is a critical component. One proposed leak, that of Na^+ influx across the plasma membrane through certain aquaporin channels, might be coupled to water flow, thus conserving energy. For the tonoplast, control of two types of cation channels is required for energy efficiency. Transporters controlling the Na^+ and Cl^- concentrations in mitochondria and chloroplasts are largely unknown and could be a major energy cost. The complexity of the system will require a sophisticated modelling approach to identify critical transporters, apoplastic barriers and root structures. This modelling approach will inform experimentation and allow a quantitative assessment of the energy costs of NaCl tolerance to guide breeding and engineering of molecular components.

I. Introduction

Soil salinity in agricultural areas is increasing world-wide due to irrigation with brackish water and to seawater encroachment on low-lying coastal regions. Its impact on crop production is further increasing as the global demand for food means agriculture extends into naturally salt-affected lands (Fig. 1a).

Salt tolerance for crop plants means the ability to grow, albeit more slowly, and produce a harvestable yield. The degree of salinity that affects crop yields depends on species, duration of exposure and the stage of crop development at which stress occurs. Saline soil (predominantly Na^+ and Cl^- salts) is defined as having an $EC_e > 4$ dS m^{-1} equivalent to 40 mM NaCl (Box 1), and in a well-drained soil would be twice this, *c.* 80 mM NaCl. This would reduce the growth of most crops by 15–20% (Munns & Tester, 2008). A higher soil salt concentration would increasingly reduce growth, but the extent of yield reduction is hard to predict as saline soils are never uniformly saline across a given area and at depth (Fig. 1b).

The precise cause of the growth reduction remains elusive – is it a pre-emptive response to conserve resources via feed-forward root signals that reduce leaf expansion and stomatal conductance, or a result of the reduction in supply of photosynthate? Is the plant adapting to conserve energy and use it more efficiently, or is a reduced supply of energy from photosynthesis limiting its growth? These principles apply to a dry soil as much as to a saline soil (Munns, 2002).

Adaptions to saline soil are many. There is a delicate balance between excluding most of the salt to avoid it concentrating in leaves and take up enough for osmotic adjustment. Plants in saline soil must exclude almost all (*c.* 98%) the salt as otherwise leaf concentrations would quickly rise to toxic concentrations (Munns *et al.*, 2020). Osmotic adjustment using Na^+ and Cl^- is 'cheaper' than using organic solutes, so long as the salt is sequestered in vacuoles whereas organic solutes provide the balancing osmotic pressure in the cytoplasm (Munns & Gilliham, 2015). Plants can avoid the high carbon (C) cost of organic solutes for osmotic adjustment by using mainly Na^+ and Cl^- but this also comes with a cost.

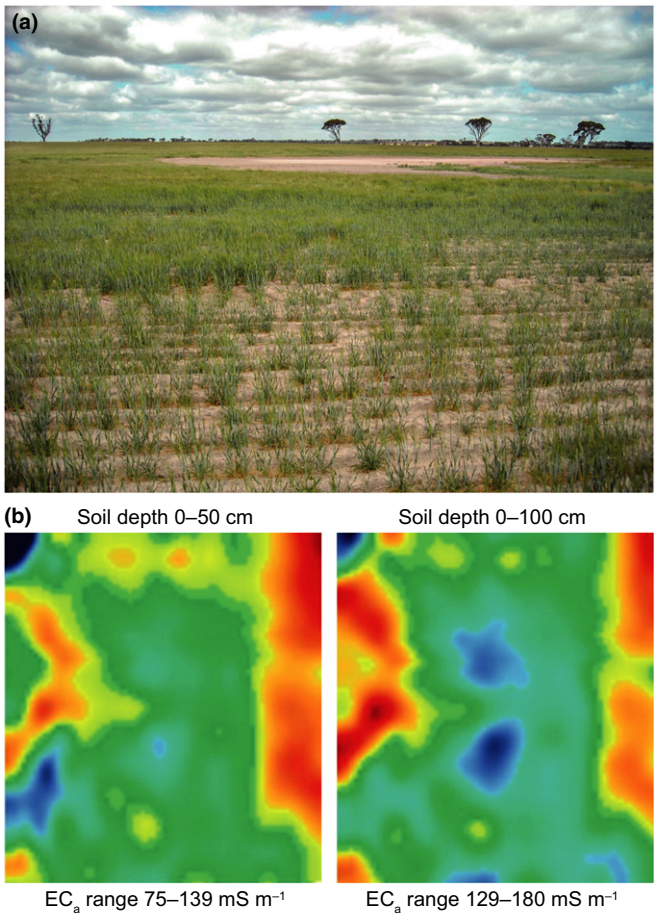

Fig. 1 Field observations of salinity. (a) Barley growing in naturally salt-affected field near Corrigin, Western Australia. Photo courtesy Stuart Roy. (b) Typical variation in soil salinity spatially and at depth. Measurements with EM38 ground conductivity meter show the apparent electrical conductivity (EC_a; mS m^{-1}) in a farmer's paddock at two soil depths (0–50 cm and 0–100 cm) at Whitwarta, South Australia. The area shown is 0.65 ha (about 80 m^2). Red, low EC_a; blue, high EC_a. Figure modified from Asif *et al*. (2018) under the terms of the Creative Commons Attribution 4.0 International License.

Box 1

Standard units and conversions

Electrical conductivity (EC): 1 dS m^{-1} = 10 mM NaCl
EC_e is EC of a saturated soil paste extract. A saturated soil has about twice the water content of a well-drained soil (at field capacity), which would decrease further during periods without rain.
EC_a is apparent EC, measured with a ground conductivity meter such as EM38. Usually given in mS m^{-1} (100 × dS m^{-1}). Must be calibrated against soil samples.
Osmotic pressure (π) = cRT (van't Hoff equation) where c is the solute concentration in Osmol l^{-1}, and RT (gas constant x temperature (Kelvin)) is 2.48 at 25°C (litre x MPa per mole). An ideal solution with osmotic potential of -0.1 MPa has 40 mOsmol l^{-1} total solutes or 20 mmol l^{-1} NaCl.

Growth parameters – for wheat or barley in moderate salinity (150 mM NaCl or 15 dS m^{-1}) in supported hydroponics

Growth rates (RGR) in saline soil: 0.1 g g^{-1} d^{-1} (Colmer *et al*., 1995; Rivelli *et al*., 2002)
Photosynthesis rates: 25–28 μmol m^{-2} s^{-1} (James *et al*., 2002; Fricke, 2017; Rawson, 1986)
Leaf respiration rates: 7 μmol $g^{-1}_{(FW)}$ h^{-1}; 0.5–1.0 μmol m^{-2} s^{-1} (Scafaro *et al*., 2017; Rawson, 1986)
Specific leaf area: 35 m^2 kg^{-1} DW (Rawson *et al*., 1987)
Conversion of leaf respiration (R) from leaf area to FW basis (from μmol m^{-2} s^{-1} to μmol $g^{-1}_{(FW)}$ h^{-1}) is therefore R × SLA ÷ FW/DW ÷ 1000 × 60 × 60
FW/DW for leaves ranges from 4 to 10 depending on species.
Typical root respiration rate: 10–25 μmol $g^{-1}_{(FW)}$ h^{-1} (Alexova *et al*., 2015; Scafaro *et al*., 2017)
ATP produced by respiration (O_2 consumption) ATP : O_2 is 4.5 (Box 2)
Root surface area : FW ratio: 70 cm^2 $g^{-1}_{(FW)}$ (W. Fricke, pers. com.)
Typical FW : DW for roots grown in hydroponics: 15 : 1 (Husain *et al*., 2004; Chen *et al*., 2005); and for roots grown in soil or for woody perennials: *c*. 10 : 1.

This review considers the costs of salt tolerance at both the whole-plant and cell levels. The costs of regulating ion and water uptake, and transport within the plant, are compared with the energy available from respiration to identify the most cost-efficient strategy, as a guide to breeding salt-tolerant crops.

II. Tissue respiration and energy supply

1. Mitochondrial ATP supply and the alternative pathway

The plant mitochondrial electron transport chain (mETC) contains two interconnected pathways with different terminal oxidases: cytochrome *c* oxidase (COX) as part of the phosphorylating, energy-conserving classical mETC, and the alternative oxidase (AOX), which together with alternative NAD(P)H dehydrogenases forms a nonphosphorylating bypass of the classical mETC (Millar *et al*., 2011; Vanlerberghe, 2013; Fig. 2). Electron transport entirely through the alternative pathway is not coupled to ATP synthesis and its operation can have a substantial impact on the efficiency of respiration by affecting the tissue ATP : O_2 ratio (Box 2; Supporting Information Notes S1). The activity of the alternative pathway *in vivo* often is stimulated by environmental stresses (Selinski *et al*., 2018), including salinity (Del-Saz *et al*., 2016). The role of the alternative pathway in plants remains uncertain but evidence suggests that it minimizes production of reactive oxygen species (ROS) in mitochondria and plays an important role in stress tolerance. In a study on the effect of salinity on Arabidopsis, both external NADH oxidation and AOX increased in capacity because of an increase in the amount of the relevant proteins (Smith *et al*., 2009). Likewise, in an analysis of the mitochondrial proteome from salt-stressed wheat, a number of

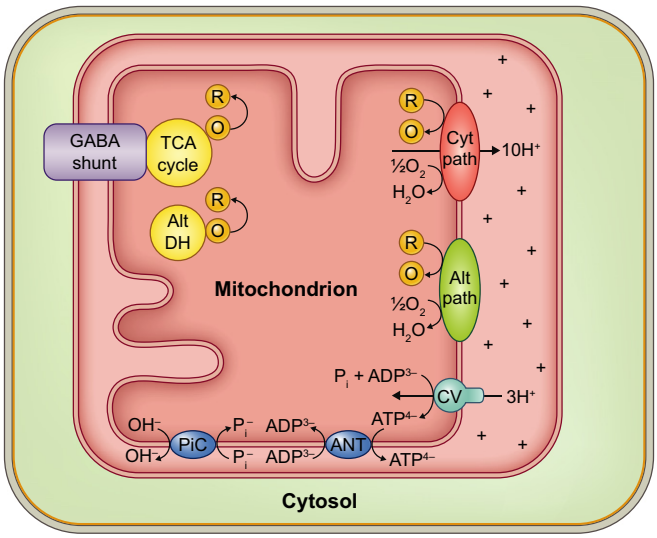

Fig. 2 The reactions and enzymes of the plant mitochondrial TCA cycle, γ-aminobutyric acid (GABA) shunt and mitochondrial electron transfer chain (mETC) linking matrix NAD^+ and NADH pools and ATP production. The GABA shunt bypasses the oxoglutarate dehydrogenase complex catalyzed step of the TCA cycle. The enzymes and complexes involved cytochrome pathway (Cyt Path) respiration (red), alternative pathway (Alt Path) respiration (green) and Complex V (CV) ATP production (light blue) and the import and export of its reactants and products (dark blue) by the adenine nucleotide translocator (ANT) and phosphate carrier (PiC) located on the inner mitochondrial membrane. This links to the pools of reductants (R) such as NADH and oxidants (O) such as NAD^+ that are recycled by the matrix TCA cycle or other alternative dehydrogenases (Alt DH). The GABA shunt (purple) includes transport steps across the mitochondrial membranes and enzyme reactions in both cytosol and matrix, which can play a part in bypassing parts of the TCA cycle that become inhibited under stress (Che-Othman *et al*., 2020).

Box 2

(a) Calculation of *in vivo* ATP : O_2 ratios (see Siedow & Day, 2000 for details)

ATP : O_2 ratios can vary *in vivo* between 5.0 and 1.75 during sucrose oxidation in plant tissues, depending on the relative contributions of the cytochrome path and the alternative pathway, which, in turn, depends on environmental conditions. Oxidation of one molecule of sucrose via glycolysis yields 4 ATP directly as well as 4 pyruvate molecules and 4 NADH for further oxidation in the mitochondria. Complete oxidation of the pyruvate and NADH in the mitochondria consumes 12 O_2 and yields a number of ATP depending on the electron transport pathway engaged. Taking into account the magnitude of the proton motive force across the mitochondrial inner membrane (typically 240 mV), $3H^+$ must move through the ATP synthase to generate an ATP molecule; the need to import Pi and ADP and export ATP consumes another H^+ equivalent, giving an H^+ : ATP of 4. Measurements with isolated mitochondria indicate that 10 H^+ are translocated out of the mitochondria for each NADH oxidized via Complex I of the mETC, giving a maximal ATP : O ratio of 2.5, and $6H^+$ for each succinate or external NADH oxidized, giving an ATP : O ratio of 1.5. From this it follows that when only the cytochrome pathway of the mETC operates, the yield of ATP from the complete oxidation of one sucrose molecule yields 60 ATP (and an ATP : O_2 of 5). If electron flow is via AOX, then this drops to 21 ATP (and an ATP : O_2 of 1.75, assuming that intramitochondrial NADH is oxidized only via Complex I rather than through the internal alternative NADH dehydrogenases). In reality, the *in vivo* ATP : O_2 ratio will be somewhere between the two extremes, depending on the relative contributions of the cytochrome path and the alternative pathway, which in turn depends on environmental conditions. For example, if the proportion of respiratory electron flow through AOX increases from 10% to 30% under salt stress, then the ATP : O_2 ratio would drop from about 4.7 to 4.

(b) Calculation of energy fixed through photosynthesis

Net CO_2 assimilation (A) can be calculated from the rates of Rubisco carboxylation (V_c) and oxygenation (V_o), and the CO_2 release from mitochondrial day respiration (R_d) using the following formula (Rawson, 1986; Walker *et al*., 2016).

$$A = V_c - 0.5\ V_o - R\mathrm{d}$$

Each Rubisco oxygenation reaction consumes 3.25 ATP and 2 NADPH, and carboxylation reaction consumes 3 ATP and 2 NADPH (Wingler *et al*., 2000; Miller *et al*., 2010). Total energy requirement per CO_2 assimilation can be calculated by summing the energy requirements oxygenation and carboxylation reactions. Taking $A = 1$ ($V_c = 1.25$, $V_o = 0.5$, $R\mathrm{d} = 0$, units of molar flux) the energy requirement will be

$$1.25\ (3\ \mathrm{ATP} + 2\ \mathrm{NADPH}) + 0.5(3.25\ \mathrm{ATP} + 2\ \mathrm{NADPH}) = 5.375\ \mathrm{ATP} + 3.5\ \mathrm{NADPH}$$

As the energy partitioning during photosynthesis and photorespiration is predictable, the requirement of ATP and NADPH can be modelled during salt stress using pre-existing resources (Walker *et al*., 2016; http://demonstrations.wolfram.com/FluxesAndEnergeticsOfPhotosynthesisAndPhotorespiration/).

antioxidant defence enzymes were increased in abundance, with AOX among the most abundant (Jacoby *et al*., 2013). AOX also may play a more general role in the homeostasis of cell metabolism by modulating TCA cycle operation under conditions where respiration is restricted by cellular energy status (Vanlerberghe, 2013), and this may be important for the synthesis of secondary metabolites, including compatible solutes under saline conditions.

In many plants, AOX synthesis is stimulated by environmental and chemical stress, although it is usually low in the absence of stress (Selinski *et al*., 2018). Inhibition of the mETC also triggers AOX synthesis, which is pertinent because high salt concentrations can inhibit cytochrome path activity in isolated mitochondria (Jacoby *et al*., 2011). In some other plants, particularly legumes, AOX protein is expressed constitutively and its activity can be substantial although subject to post-translational regulation by mitochondrial redox status and the presence of certain organic acids, especially pyruvate (Selinski *et al*., 2018). In legumes, AOX contribution to respiration varies depending on tissue and developmental stage, and the imposition of stresses such as drought and salinity. It can be very significant, leading to decreases in ATP concentrations *in vivo* (Millar *et al*., 1998; Ribas-Carbo *et al*., 2005; Del-Saz *et al*., 2016). Mitochondria isolated from most species readily oxidize exogenous NADH, but we know little about the regulation of the alternative NAD(P)H dehydrogenases *in vivo*. Some of the alternative NADH dehydrogenases are transcriptionally responsive to salt stress (Smith *et al*., 2009), and the oxidation of external NADH is stimulated by salt in isolated mitochondria. The oxidation of malate, pyruvate, succinate and glutamate, however, is inhibited, indicating a differential effect of salt on tissue respiration depending on the substrate respired (Jacoby *et al*., 2016).

Relatively few accurate studies on the *in vivo* contribution of AOX to respiration have been made, mainly because of the difficulty involved in these studies. Accurate estimations require mass spectrometry to measure ^{18}O discrimination between AOX and COX (Del-Saz *et al*., 2017). Because AOX activity has the potential to severely impact respiratory efficiency, it is important that more *in vivo* measurements of AOX engagement in a variety of species under saline conditions are made if we are to fully understand the energetics of salt tolerance.

2. Sources of NADH for tissue respiration

Tissue respiration is at the centre of plant metabolic networks as the TCA cycle links it to both C and nitrogen (N) metabolism and

supplies much of the NADH required to maintain ATP supply (Nunes-Nesi *et al.*, 2013). Salt inhibition of the TCA cycle could activate alternative metabolic routes, including the gamma-aminobutyric acid (GABA) shunt pathway (Krasensky & Jonak, 2012; Nunes-Nesi *et al.*, 2013). The GABA shunt bypasses the oxoglutarate dehydrogenase complex (OGDC) catalysed Julkowska of the TCA cycle (Fig. 2), producing glutamate that enters the mitochondria for further catabolism (Che-Othman *et al.*, 2020; Fig. 2). The GABA shunt is thought to be important in stress adaptation in plants by regulating cytosolic pH, limiting ROS production, regulating N metabolism and bypassing steps in the TCA cycle (Carillo, 2018). Links are suggested between salinity exposure and activity of the GABA shunt (Che-Othman *et al.*, 2017), but the exact mechanism of induction and its consequences for tissue respiration are only just starting to be revealed (Che-Othman *et al.*, 2020).

In addition to TCA cycle enzymes and Glycine Decarboxylase Complex (GDC), it is likely that alternative sources of NADH may become significant under exposure to salinity. The induction of other dehydrogenases is observed in other stresses, where amino acids are broken down and increases are seen in branched chain amino acid catabolism enzymes (Peng *et al.*, 2015). Some of these dehydrogenases have been shown to contribute electrons directly to the ubiquinone pool of the mETC, effectively bypassing Complex I and consequently altering ATP synthesis. Improving our understanding of these different metabolic pathways will be required if we are to fully understand the implications of salinity exposure on NADH supply and mitochondrial ATP production.

The contribution of beta-oxidation of fatty acids to energy supply during salt stress is unknown, but we do not consider it likely to play a major role in plant adaptation to this stress. The participation of mitochondria in this process in plants is controversial and it is generally assumed that most beta-oxidation occurs in the peroxisomes. The extent to which this contributes to ATP production is likely to depend on species and tissue, and has not been investigated to our knowledge. More work is needed, especially under saline conditions.

3. Vacuolar proton-pumping pyrophosphatases provide additional energy sources for salinity tolerance

High-energy phosphate containing molecules other than ATP can be used for energizing processes. Vacuolar pyrophosphatases

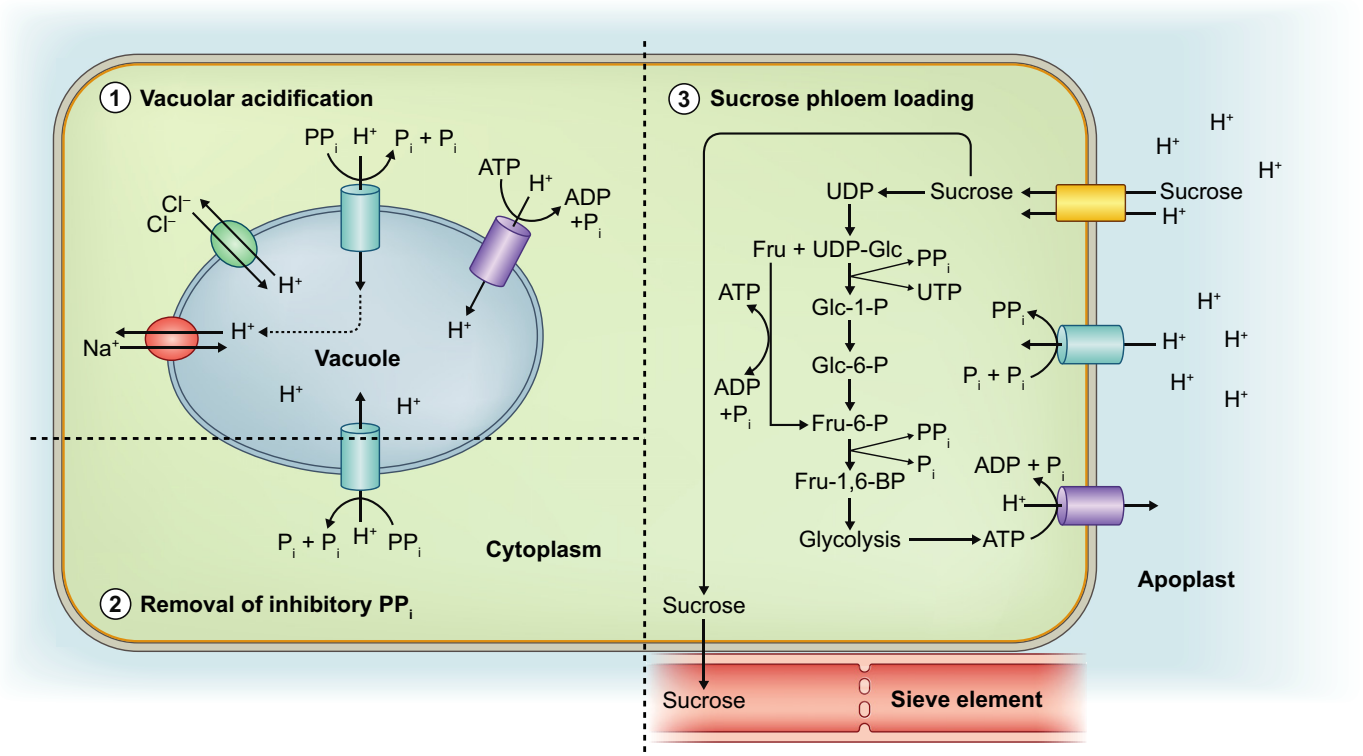

Fig. 3 A variety of roles for the vacuolar proton-pumping pyrophosphatase. A generic plant cell showing the variety of ways the vacuolar proton pumping pyrophosphatase (H^+-PPase) can provide an alternative source of energy during salinity stress. (1) Vacuolar acidification. Localized to the tonoplast, the vacuolar H^+-PPase (blue) will use energy released from the hydrolysis of PPi to orthophosphate (Pi) to pump protons (H^+) into the vacuole. Along with vacuolar ATPases (purple), vacuolar H^+-PPases establish an electrochemical potential for H^+ across the tonoplast, which is used by other vacuolar transporters (red & brown) to sequester Na^+ and Cl^- into the vacuole. (2) Removal of inhibitory pyrophosphate (PPi). Vacuolar H^+-PPases regulate PPi concentrations in the cytosol. Accumulation of PPi in the cytosol, particularly in younger tissues, can inhibit PPi-dependent metabolic pathways, such as gluconeogenesis and the Smirnoff–Wheeler pathway. (3) Enhancing sucrose transport from source to sink tissues. In phloem companion cells, H^+-PPases are shown to be localize to the plasma membrane, where it is hypothesized they synthesize PPi from orthophosphate. This additional PPi is used to enhance sucrose metabolism in these cells, thereby generating more ATP to pump protons into the apoplast which can be used by sucrose transporters, ultimately enhancing sucrose transport into sieve elements. Not all of these processes will be occurring in all cells at all times, and some may be cell-type specific. Figure modified from Khadilkar *et al.* (2016) and Schilling *et al*. (2017).

(Vacuolar H^+-PPase, EC.3.6.1.1) pump protons across the tonoplast into vacuoles (Gaxiola *et al.*, 2016; Schilling *et al.*, 2017), using pyrophosphate (PPi) as an energy source (Fig. 3). They work together with vacuolar H^+-ATPases to acidify the vacuole (Kriegel *et al.*, 2015; Schilling *et al.*, 2017). Plants with high expression of vacuolar H^+-PPases have significant abiotic stress tolerance, including salinity tolerance (Gaxiola *et al.*, 2016; Schilling *et al.*, 2017).

Vacuolar H^+-PPases may be particularly important when ATP supply is limited during abiotic stress. A significant portion of vacuolar acidification may be generated by non-ATPase pathways and used by Na^+/H^+ and Cl^-/H^+ antiporters to sequester Na^+ and Cl^- in the vacuole as part of a tissue tolerance mechanism (Li *et al.*, 2006; Kriegel *et al.*, 2015; Nguyen *et al.*, 2016). H^+-PPases are dependent on potassium ions (K^+), thus K retention in the cytoplasm under salinity may be critical for their function (Shabala *et al.*, 2014). H^+-PPases have been shown more recently to be involved with rapid mobilization of sugars and carbohydrates from source to sink tissue (Pizzio *et al.*, 2015; Gaxiola *et al.*, 2016), and in faster metabolism of sugars in cells (Ferjani *et al.*, 2012). Both processes will contribute to enhancing a cell's energy budget.

4. Energy supply from photosynthesis

Photosynthesis supplies energy in the form of reduced C to fuel growth and maintenance. In the majority of crop plants, salt stress decreases photosynthesis by (1) reducing CO_2 uptake through stomata (Rawson, 1986; Delfine *et al.*, 1999; James *et al.*, 2002), (2) causing ionic (Na^+, K^+, Cl^-) imbalance within the chloroplasts, resulting in poor efficiency of light and dark reactions (Delfine *et al.*, 1999; Percey *et al.*, 2016; Bose *et al.*, 2017), and (3) causing oxidative damage to photosystems and membranes (Miller *et al.*, 2010; Bose *et al.*, 2014). However, the extent of the decrease in photosynthesis under salinity varies widely among crop species and genotypes. In tolerant genotypes that are able to keep salt out of the leaf, photosynthetic supply is not affected. In such cases, the decrease in potential growth (compared to a nonsaline control) must be directly proportional to, and a measure of, the energy cost associated with tolerance.

5. How to estimate the energy cost of CO_2 fixation during salt stress

In a nonlimiting environment (e.g. absence of photorespiration), three ATP and two NADPH are required per CO_2 assimilated (Wingler *et al.*, 2000). This demand can be met through absorption of four photons each by PSII and PSI and subsequent linear transport of four electrons from PSII to PSI (Kramer & Evans, 2011). Under salt stress there is an increase in energy demand for CO_2 assimilation due to an increase in photorespiration (Wingler *et al.*, 2000), protein turnover to repair and strengthen photosystem components (e.g. energy cost to import a protein into chloroplasts is *c.* 650 ATP; Miller *et al.*, 2010; Shi & Theg, 2013), and ion transport activity to maintain an optimum ionic environment within the chloroplasts (Bose *et al.*, 2017). For example, during photorespiration, each oxygenation reaction consumes 3.25 ATP and 2 NADPH (Wingler *et al.*, 2000). Photorespiration can occur at *c.* 25% the rate of net CO_2 assimilation (25°C, $CO_2 = 350$ ppm; Walker *et al.*, 2016), which will increase the consumption of ATP and reducing equivalents per CO_2 fixed from 3 ATP and 2 NADPH to 5.375 ATP and 3.5 NADPH (Box 2; Notes S1).

In order to meet the high energy demand during salt stress, chloroplasts could increase ATP production by altering the H^+ : ATP ratio required by the ATP synthase or engaging with cyclic electron flow around PSI, using the water–water cycle, the malate valve and plastoquinol oxidase (Kramer & Evans, 2011). Among these mechanisms, enhanced cyclic electron flow around PSI has been shown to increase ATP production during salt stress, and the excess ATP generated has been suggested to fuel ion transport mechanisms that prevent salt over-accumulation into the chloroplasts (He *et al.*, 2015). Under control conditions cyclic electron flow amounts to 14%; whether it increases or not under saline conditions is important to know.

III. Water and ion transport

Membranes are inherently high energy barriers for water and ion transport. For energetics of salinity tolerance, any combined flux of Na^+ and Cl^- across either plasma membrane or tonoplast and resultant feedbacks for maintenance of electroneutrality and negative membrane potential will entail energy costs to the cell. Elevated fluxes of Cl^- and Na^+ under salinity stress will affect most other transport due to changes in membrane potential and pH (due to proton-coupled transport). For water, control can be exerted and much higher permeability obtained via the operation of aquaporins (Maurel *et al.*, 2015). Aquaporins are linked to cell energetics (Chaumont & Tyerman, 2014), respond in a complex way to salinity (Boursiac *et al.*, 2005, 2008; McGaughey *et al.*, 2018), and some may allow ion permeation (Byrt *et al.*, 2017; Kourghi *et al.*, 2017). Changes in water permeation will influence Na^+ and Cl^- fluxes by virtue of their coupling by convection in the transpiration stream and in radial transport across the root (Foster & Miklavcic, 2016, 2017).

In previous estimates of energy costs of ion fluxes in roots, the paradigm used is the number of membranes crossed and the number of protons consumed, which can then be converted to ATP demand based on stoichiometry of protons pumped per ATP hydrolysed (usually taken as 1 : 1; Venema & Palmgren, 1995; Kurimoto *et al.*, 2004; Malagoli *et al.*, 2008). Some isotope flux calculations indicate that energy costs approach the ATP produced by respiration (e.g. Malagoli *et al.*, 2008 for rice), although subsequent publications have questioned these results (Britto & Kronzucker, 2015; Flam-Shepherd *et al.*, 2018; Munns *et al.* 2020). These estimates are just for Na^+ in isolation and ignore the Cl^- ion and feedback effects on other fluxes, such as loss of K^+ (Cuin *et al.*, 2008) and NO_3^- (Teakle & Tyerman, 2010). Just the stoichiometry of the proton pump could have a profound effect on the energetics, and an H^+ : ATP < 1 (e.g. when the pump is not activated (Pedersen *et al.*, 2018)) would reduce the energy efficiency substantially; it is interesting that cytosolic K^+ and potentially Na^+ can have an effect on this (Buch-Pedersen *et al.*,

2006). The identification of molecular components of energetically costly processes can be used to engineer plants for improved yield (Amthor *et al.*, 2019).

1. Ways of calculating energy of transport

Energy budgets When considering a plant that tolerates salinity, we can ask many questions about how it manages in terms of energy (Amthor, 2000; Bijlsma *et al.*, 2000; Kooijman & Troost, 2007; Munns & Gilliham, 2015). Ideally, we want to know the total energy that is (1) captured, (2) expended on biochemical work including growth, maintenance of metabolism and respiration, and (3) invested in salt tolerance. Obtaining data on (1–3) is one thing; interpreting these data, is another. For example, if the energy drain is large, we may conclude that the responses come at high cost and, because they require such a large portion of energy, must be important. Yet, we could also argue that the responses are unlikely to operate over the long term, because they are so costly. It is desirable to include any component processes (Raven, 1985; Assmann & Zeiger, 1987; Bloom *et al.*, 1992; Scheurwater *et al.*, 2000), for example synthesis of transport proteins, in the energy budget of the overall process. However, in practice this is difficult to achieve, and it is easier to consider a well-defined start and endpoint of the process. We apply this rationale here to solutes in the first instance.

Energising solute movement The energy of a solute X, such as a mineral nutrient ion, can be quantified by the electrochemical potential of that solute (μ_X). The energy which is released by or required for the movement of X from soil (S) into a leaf cell (L) is $\Delta\mu_X(SL) = \mu_X(L) - \mu_X(S)$, with $\Delta\mu_X(SL) < 0$ for a spontaneous movement of X down a gradient in energy, and $\Delta\mu_X(SL) > 0$ for a movement of X energetically-uphill (for calculations, see Fig. 4).

There are five options for how to approach such an energy calculation. Option 1: we ignore all transport steps between S and L and only consider the start and endpoint of μ_X. Option 2: we consider all of the intermittent steps of transport. Option 3: we render the second option more complete and more complicated, by including transport across intracellular membranes, particularly the tonoplast. Option 4: we ignore the chemical nature of solute X and link its movement to the energization of transport processes across the plasma membrane through the plasma membrane H^+-ATPase (PM-H^+-ATPase); we also ignore intermittent transport steps. One H^+ needs to be pumped at least for every solute moved from S to L (at least one membrane crossing event) so we base our energy calculation on the proton motive force (pmf; Palmgren, 2001; Fricke, 2017). Option 5: we include the energy which is required to synthesize/maintain the biomolecules (e.g. membrane transporters) and cellular processes (e.g. trafficking) that are required to support the transport steps (Raven, 1985). This approach is the most complete one, yet the difficulty is that all processes in a cell are somehow interconnected and should be considered. This is not possible to do as yet.

Option 1 provides the lowest estimate of energy for solute movement from S to L. This applies particularly to the situation under salt stress (high external Na^+ and Cl^-). We deal with a cation and anion, each crossing plasma membranes with a significantly negative (inside) membrane electrical potential (Cuin *et al.*, 2003). This should favour uptake of Na^+, even if it was as support of the co-transport of another solute (e.g. K^+) into cells (Carden *et al.*, 2001, 2003; Cuin *et al.*, 2003). By considering the chemical nature of each solute we 'save' energy (Fricke, 2020 – see current feature issue). Any intermediate transport between S and L causes 'frictional' loss of energy through heat. By omitting intermediate transport steps while taking the chemical nature of solute

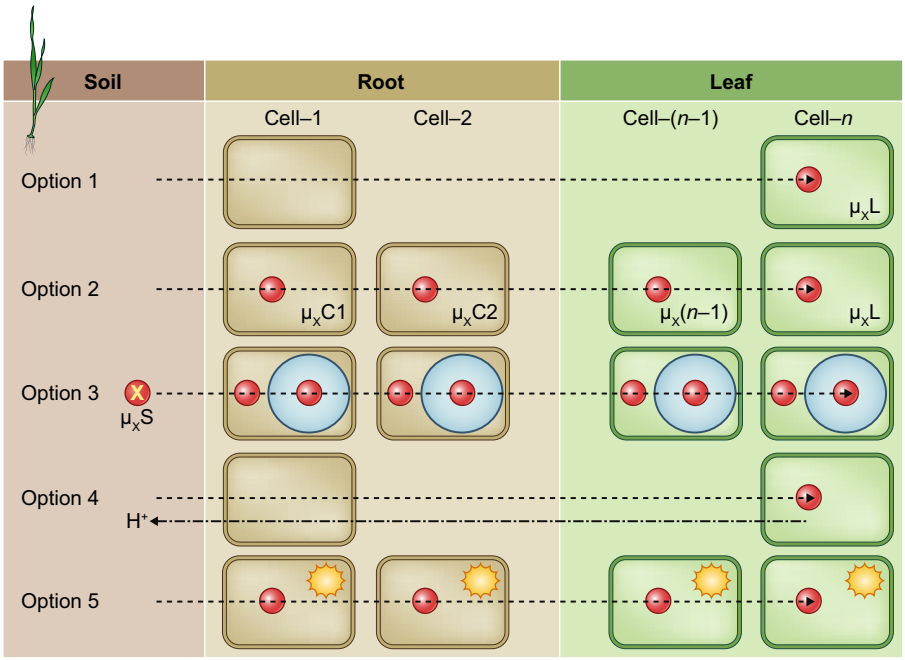

Fig. 4 Five possible ways to calculate the energy associated with the movement of solutes from a soil location to target location in leaf. The options shown are not exhaustive. For details, see text. Explanation of symbols and abbreviations: red circle with X, solute species X; $\mu_X S$, chemical potential of solute X in compartment S (soil); other compartments are leaf (L) or cells (C) at the start (C1) or end (Cn) of transport path of solute; yellow symbol, energy associated with providing cellular infrastructure for transport, such as synthesis and regulation of transporter protein; H^+, proton pumping through the plasma-membrane-localized H^+-ATPase; blue circular lines, tonoplast depicting the large central vacuole. The picture shows a 16-d-old barley plant.

Box 3 Calculation of minimum costs of NaCl accumulation in leaf and root vacuoles of a wheat plant growing in a saline soil of 150 mM NaCl and comparing effect of leaks

NaCl concentration in vacuole = 150 mM
Growth rate = 0.1 d^{-1}
Shoot : root ratio = 1.3 (Van Den Boogaard *et al*., 1996)
Leaf resp. = 7 μmol $g^{-1}_{(FW)}$ h^{-1} Root resp. = 10 μmol $g^{-1}_{(FW)}$ h^{-1}
Plant C used in root resp. = 16%; Plant C used in leaf resp. = 13% (Van Den Boogaard *et al*., 1996)
$H^+/Na^+ = 1$, $H^+/Cl^- = 2$, $H^+/ATP = 1$
$ATP/O_2 = 4.5$
If leak present = 0.5 × net flux

Pathway: One way to leaf via xylem through roots (no bypass flow, Fig. 5)
Na^+ Root: 2 membranes, outside → symplast passive, symplast → xylem active
Leaf: 2 membranes, xylem → leaf symplast passive, symplast → vacuole active
Cl^- Root: 2 membranes, outside → root symplast active, symplast → xylem passive
Leaf: 2 membranes: xylem → leaf symplast active, symplast → vacuole passive

Total costs for Na^+ + Cl^- transport
No leaks:
Leaf %ATP used = 7.1%
Root %ATP used (including for leaf supply) = 11.4%
% of root C used = 1.8%
% of leaf C used =0.96%
Total % plant C used = 2.76%

Leak (0.5 × net flux) at one membrane (root and leaf)
Leaf %ATP used = 14.2%
Root %ATP used (including for leaf supply) = 22.8%
% of root C used = 3.7%
% of leaf C used = 1.9%
Total % plant C used = 5.6%

Leak (0.5 × net flux) at two membranes (root and leaf)
Leaf %ATP used = 28.3%
Root %ATP used (including for leaf supply)= 45.6%
% of root C used = 7.4%
% of leaf C used = 3.8%
Total % plant C used = 11.2%

Note: These figures do not account for maintenance of membrane potential and do not include a small correction for respiration related to relative growth rate. They also do not include a contribution from the H^+-PPase at the tonoplast that would reduce costs. Cl^- uptake from high salt soil may be passive (Fig. 5).

X into account, we obtain a lowest-cost estimate for solute accumulation.

Cost estimates If the cost estimate for solute movement exceeds the energy available from C assimilation (day) or dark respiration (night), we have to question our assumptions on energy budgets; if the cost estimate is well within the energy available, it does not mean that our energy budgets and assumptions are correct, but we can conclude that this solute movement is theoretically possible. We also can compare our lowest-cost estimate with the minimum energy required to establish turgor pressure in cells, which results from accumulation of solutes and associated water uptake. Turgor pressure has many functions in cells (Beauzamy *et al*., 2014), and it also presents some energy, as 1 MPa of hydrostatic pressure corresponds to 10^6 J m^{-3}. In Box 3, calculations of energy requirements are made for transport of Na^+ and Cl^- from a saline soil solution to leaf vacuoles of a wheat plant that is accumulating 150 mM NaCl in order to osmotically adjust during growth. It is based on Option-4 (Fig. 4) but including minimal (not all) transport steps in the pathway and different possibilities that may occur at these steps with respect to leaks (Fig. 5). These are compared with rates of respiration in order to assess the proportion of energy available that is used in transport. This exercise serves to illustrate the magnitude of energy required as well as some of the parameters that are required, particularly the leaks across membranes in the pathway that can substantially increase the energy required. These leaks are dealt with further in the following sections.

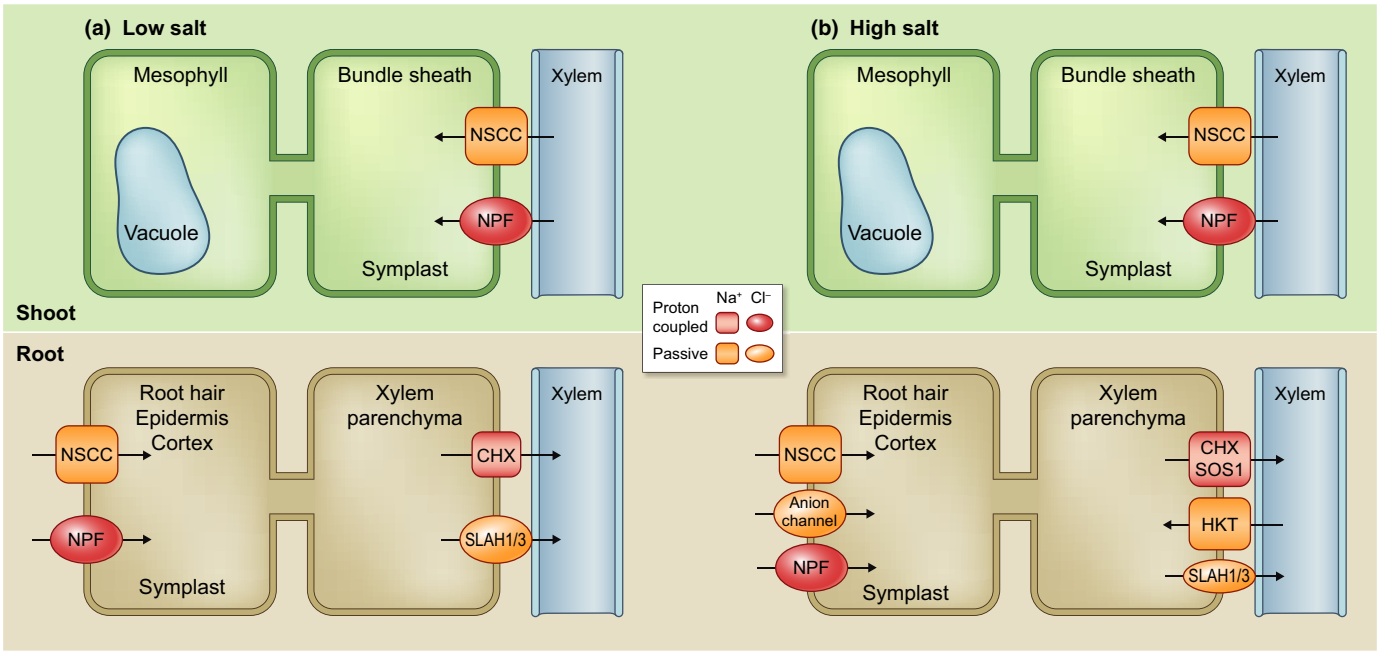

Fig. 5 Active and passive membrane steps for the long-distance transport of Na^+ and Cl^- in plants under high and low salt concentrations. (a) Under low salt, Cl^- enters the root and shoot symplast actively through a $1Cl^-$: $2H^+$ symporter (e.g. ZmNPF2.6), and is loaded towards the xylem by channel-mediated passive transport (e.g. SLAH1/3 heteromer). Na^+ enters the symplast passively via nonselective cation channels (NSCC), and is effluxed via active proton exchange (e.g. through CHX or similar mechanism). (b) Under high salt, Cl^- may enter the root symplast by passive transport, whereas passive Cl^- efflux to the xylem (though SLAH1/3 heteromer) is downregulated at the transcriptional level. Na^+ exclusion from the root xylem into the symplast is likely to be mediated passively by HKT proteins. Apoplastic barriers in the root (not shown) are important to restrict by-pass flow of NaCl to the xylem. As ion exclusion is controlled mostly at the root level, it is expected that re-uptake into the shoot symplast is similar under low and high salt. Cl^- will accumulate preferentially in leaf epidermal cells (Leigh & Tomos, 1993), but the mechanism for this remains unclear. A final transport step in to the vacuole of leaf cells would involve active transport of Na^+ and passive or active transport for Cl^- (Fig. 3).

2. Energetics of Na^+ transport: a conundrum

Current dogma suggests that acquisition of nutrient and toxic ions by plant root cells is controlled mainly by influx and efflux transporters residing in the plasma membranes. Bypass flow can occur via the apoplast in rice depending on the development of lateral roots and apoplastic barriers (Krishnamurthy *et al.*, 2011). This would be important to consider in energy calculations considering that it avoids 'expensive' membrane steps, but control on fluxes is presumably more limited. The difference between unidirectional influx and efflux at the plasma membrane is the 'net flux'. In general, radiotracer experiments show that, as external ion concentrations increase, so do influx and efflux, whereas net fluxes remain low, indicating rapid cycling of ions (Britto & Kronzucker, 2006).

In the Rapid Transmembrane Sodium Cycling (RTSC) model of Na^+ transport in plants (Britto & Kronzucker, 2015), Na^+ initially enters the root cells passively down its electrochemical gradient due to a negative inward membrane potential (−80 to −120 mV), with an assumed cytoplasmic Na^+ concentration ($[Na^+]_{cyt}$) of between 10 and 30 mM (Munns & Tester, 2008), significantly less than $[Na^+]_{ext}$ under saline conditions. Genetic variation for unidirectional influx exists, as salt-tolerant species such as *Suaeda maritima* and *Spergularia marina* have lower influxes than salt-sensitive species such as rice, wheat or Arabidopsis (Cheeseman *et al.*, 1985; Wang *et al.*, 2007). Na^+ then exits the cell, at nearly the influx rate, via active transport across the plasma membrane. Efflux measurements are notoriously difficult to perform accurately via radiotracer techniques (Volkov, 2015).

Several transporters that could allow Na^+ influx have been proposed, some based only on physiological characteristics, including voltage-independent nonselective cation channels (vi-NSCCs; Demidchik & Maathuis, 2007), AtPIP2;1 (an aquaporin as a candidate for vi-NSCCs; Byrt *et al.*, 2017), AKT1 (K^+ channel), LCT1 (low-affinity cation transporter), HKT-type (Na^+ and/or K^+ transporters), KUP/HAK/KT (K^+ transporters) and CCC (cation-Cl^- cotransporter) dependent on location and co-transported ion gradients (Kronzucker & Britto, 2011). However, only SOS1 has been proposed as an apparent efflux transporter, although it may participate in internal Na^+ transport and perhaps only mediates Na^+ efflux from root tips where cell Na^+ concentrations remain low, presumably to protect meristematic cells (Kronzucker & Britto, 2011). This may be genotype- and Ca^{2+}-dependent (Wu *et al.*, 2015). The vi-NSCCs could allow passive efflux if the electrochemical gradients are appropriate (McGaughey *et al.*, 2018). Future progress in development of crop cultivars with improved Na^+ transport traits will benefit from resolving the molecular identity of key Na^+ transporters.

The energy requirements for sustaining influx and efflux of Na^+ across the plasma membranes of root cells proposed by tracer experiments would result in a very large energy burden if it involves a Na^+/H^+ antiporter (e.g. SOS1), because for every Na^+ effluxed

across the plasma membrane, one H^+ must be extruded via the H^+-ATPase. Further, for every H^+ extruded one ATP is hydrolyzed, assuming optimal coupling to ATP, and the ratio of ATP produced per O_2 consumed is 4.5 (Boxes 1 and 2). This would mean that, at most, 4.5 Na^+ can be extruded for every O_2 consumed in respiration. Estimates for maximal whole root respiration (expressed as O_2 consumption) are generally in the range of 10–25 μmol $g^{-1}_{(FW)}$ h^{-1} (Box 1). Consequently, sustaining many of the measured (or calculated) Na^+ effluxes would require more ATP than produced by the entire maximal respiration of the root (Britto & Kronzucker, 2009). This problem was described initially for Cl^- fluxes in relation to respiration in frog epithelia and has been referred to as Ussing's conundrum (Ussing, 1947, 1994; Britto & Kronzucker, 2009). Ussing (1994) suggested that the flux of one ion in the energetic 'uphill' direction may be coupled to the flux of another ion in the 'downhill' direction. This suggests that measurement of Na^+ fluxes in isolation will be prone to artefact as it does not consider the energetic effects of flux via other transporters (e.g. Cl^-; Colmenero-Flores *et al.*, 2007).

Measurements of Na^+ influx via radiotracer techniques assume that the flux measurement is indeed trans-membrane, yet it is possible that apoplastic binding or exchange of the tracer creates an overestimate of the true Na^+ influx (Britto & Kronzucker, 2015; Munns *et al.*, 2020). There are several techniques to measure Na^+ fluxes, each with advantages and disadvantages (Volkov, 2015). Gaining accurate measures of cytosolic ion concentrations is challenging, because of the very small volume of cytosol, yet this resolution is needed to model Na^+ fluxes (Foster & Miklavcic, 2017). It also is clear that the contribution to Na^+ uptake of alternate pathways, such as 'bypass flow', and the influence of the epidermis, multiple cortical layers and the root endodermal barriers on root radial transport, must be better understood (Yeo *et al.*, 1987; Flam-Shepherd *et al.*, 2018). Ultimately though, determination of the molecular identity of the transporters mediating Na^+ transport in plant roots will be required to dissect the system and provide targets for efforts to develop cultivars with superior Na^+ transport traits.

Leakage of Na^+ across the tonoplast Salinity tolerance of tissues is critically dependent on efficient vacuolar Na^+ sequestration. Although the mechanisms of Na^+ transport into the vacuole are still a matter of debate (Bassil *et al.*, 2011), tonoplast-based NHX Na^+/H^+ exchangers are considered likely candidates (Bassil *et al.*, 2019). However, active removal of Na^+ from cytosol to vacuole is only one component of vacuolar sequestration. Another often-neglected component is Na^+ retention in vacuoles. This retention is based on an efficient control of Na^+-permeable vacuolar channels that mediate the back-leak of Na^+ into the cytosol and, if not regulated tightly, may result in a significant energy cost.

Two major types of Na^+-permeable channels are present in the tonoplast (Isayenkov *et al.*, 2010). The slow-activating (SV) channels are permeable to both mono- and divalent cations, and fast-activating (FV) channels that are permeable to monovalent cations only (Pottosin & Dobrovinskaya, 2018). Although the molecular identity of FV channels remains unknown, SV channels are encoded by a TPC1 ('two-pore channel 1′) protein (Hedrich *et al.*, 2018). Both channels are ubiquitous and abundant in patch clamp experiments on vacuoles (Pottosin & Schnknecht, 2007; Demidchik *et al.*, 2018). Being nonselective, these channels do not discriminate between Na^+ and other cations. As SV channels allow the release of K^+ from the vacuole, they are essential for maintaining cytoplasmic K^+ homeostasis (Hedrich *et al.*, 2018). Their relative expression determines the vacuolar Ca^{2+} storage capacity (Gilliham *et al.*, 2011). Also, TPC1 channels play a key role in generating Ca^{2+} waves in long-distance signalling in plants, including those under saline conditions (Choi *et al.*, 2014). These channels may need to be open for normal cell metabolism and signalling, but salinity tolerance may require them to be closed most of the time. Model calculations (Shabala *et al.*, 2020) show that if each cell has only one open SV channel at a given time, the back-leak may approach 100% of the influx. For *in planta* conditions (at resting cytosolic Ca^{2+} concentrations) the measured SV currents are *c.* 10 pA per vacuole (Perez *et al.*, 2008), which equates to approximately five open SV channels. This could mean that all available energy may be wasted in cycling of Na^+ in and out of the vacuole. Halophytes have developed an ability to reduce the number of open SV channels by several fold when grown under saline conditions (Bonales-Alatorre *et al.*, 2013), by an unknown mechanism. This needs to be addressed in future studies to enable plant breeders to target reduced Na^+ cycling across the tonoplast.

3. Transport of Na^+ and Cl^- from soil to leaf

The cell-mediated pathway for Na^+ and Cl^- transport from soil to shoot (i.e. neglecting bypass flow in the root) involves at least three plasma membrane components: (1) entry at the root symplast, (2) unloading towards the xylem apoplast, (3) re-entry at the shoot symplast; and finally crossing the tonoplast membrane for vacuolar sequestration (Fig. 4). For Na^+, our present understanding of electrochemical gradients and transport mechanisms for the plasma membrane favours only a single energy-requiring step: efflux to the xylem apoplast, notwithstanding the secondary effects on other ions caused by passive Na^+ entry, such as depolarization of the membrane potential and requirement for charge balance (Fig. 5a). For root-to-shoot Cl^- transport, a minimum of two energy-requiring plasma membrane transport steps are required, at least under the normal paradigm that Cl^- entry is via proton co-transport, although it is possible for Cl^- to enter the symplasm passively at high external Cl^- concentrations depending on the membrane potential (Teakle & Tyerman, 2010). These steps include uptake at the root symplast and re-uptake at the shoot symplast (Fig. 5a). In reality, it is possible that a multitude of Na^+ and Cl^- pathways exist; for example, Na^+ storage may occur in xylem parenchyma cells as a consequence of HKT mediated transport (Munns *et al.*, 2012).

Entry into the root symplast Passive influx of Na^+ from the soil solution into the cytosol of root epidermal and cortical cells (Cheeseman, 1982; Fig. 5a) is likely achieved through NSCC (Tyerman *et al.*, 1997; Davenport & Tester, 2000; Demidchik & Tester, 2002). Sub-sets of plasma membrane water channels such as the Arabidopsis PIP2;1 and PIP2;2 aquaporins, which are

abundant in root epidermal cell plasma membranes and are permeable to Na^+, have been proposed as candidates for NSCCs (Byrt *et al.*, 2017; Kourghi *et al.*, 2017); these aquaporins qualitatively and semi-quantitatively match the NSCC properties as measured in isolated root protoplasts by patch-clamp (McGaughey *et al.*, 2018).

Chloride can enter the plant root symplast through secondary active transport either coupled to H^+ uptake or, at high salinity, passively due to an initial membrane depolarization (Skerrett & Tyerman, 1994; Lorenzen *et al.*, 2004; Saleh & Plieth, 2013; Fig. 5b). $Cl^- : H^+$ symport is likely to occur across only one membrane, which may be plasma membranes of root hairs, epidermal cells or cortical cells (Fig. 5a). Symport of $1Cl^- : 2H^+$ has been identified in plant root hairs (Felle, 1994), and the expression of *ZmNPF2.6* – which encodes a protein with $1Cl^- : 2H^+$ activity – was detected in the plasma membranes of maize root epidermal and cortical cells (Wen *et al.*, 2017).

Once in the symplast, radial Na^+ and Cl^- movement towards the xylem may occur through plasmodesmata, with no membrane steps required. However, cycling in and out of cells and vacuoles along the way may occur.

Xylem loading and retrieval Sodium transport to the xylem is an energy-requiring step, most likely coupled to H^+ antiport, and could occur via a Na^+–H^+ exchange with the acidic apoplast. Numerous candidate proteins might catalyze this Na^+ transport step in plants, for example SOS1 and CHXs (Shi *et al.*, 2003; Zhu *et al.*, 2019; Fig. 5a).

Chloride entry to the xylem apoplast is channel-mediated by SLAH1 and SLAH3 (Cubero-Font *et al.*, 2016). Expression of *SLAH1* and *SLAH3* is downregulated by salt and abscisic acid (ABA), and a *slah1* mutant has reduced Cl^- in shoots under NaCl treatment compared to wild-type (Cubero-Font *et al.*, 2016; Qiu *et al.*, 2017). Although no energy *per se* is required for this step (Fig. 5a,b), energy will be required for maintenance of membrane potential, because high efflux of Cl^- will depolarize the membrane. Aluminium-activated malate transporters (ALMT) that can function as Cl^- channels also may release anions to the xylem (B. Li *et al.*, 2017).

Retrieval of Na^+ from the xylem is mediated by HKT1-type transporters (Davenport *et al.*, 2007; Munns *et al.*, 2012; Xu *et al.*, 2019). Some HKT proteins have been shown to function as Na^+/K^+ symporters at micromolar Na^+ concentrations. However, at millimolar Na^+ concentrations, as would be expected in the xylem apoplast under salt stress, HKT proteins display channel-like Na^+ uniporter activity (Munns *et al.*, 2012; Henderson *et al.*, 2018). Thus, xylem retrieval of Na^+ is likely to be passive under salt stress (Fig. 5b). The Na^+ retrieved by HKT1 is effluxed from the upper part of the root (Davenport *et al.*, 2005).

Re-entry to the shoot symplast and movement into the mesophyll cells The pathway for Na^+ entering the shoot symplast from the xylem apoplast and then moving into mesophyll cells could be via NSCCs, perhaps Na^+-permeable aquaporins in the plasma membrane of bundle sheath cells (Shatil-Cohen *et al.*, 2011; Sade *et al.*, 2014; Fig. 5a,b). Chloride re-enters the shoot symplast from the xylem apoplast at the plasma membrane of bundle sheath cells via secondary active transport. The maize $1Cl^- : 2H^+$ symporter *ZmNPF2.6* shows preferential expression in bundle sheath cells (Wen *et al.*, 2017), suggesting that a NPF protein family member catalyzes this active Cl^- influx in leaves. Once in the shoot symplast, Cl^- can move into mesophyll cells through plasmodesmata where it can accumulate to high concentrations, yet accumulates, preferentially, to much higher concentrations in the epidermis in moderately salt-tolerant barley (Dietz *et al.*, 1992; Fricke *et al.*, 1994, 1996).

Although passive Na^+ and Cl^- transport is considered to be energy-free, the electrochemical gradient that drives passive ion flux is generated by an energy-dependent mechanism (the H^+-ATPase). Hence changes in the functioning of the H^+-ATPase under salinity would influence both passive and active Na^+ and Cl^- transport. Osmotic stress, including from NaCl, increases the coupling ratio (that is more proton efflux per ATP hydrolysed) of the H^+-ATPase (Kerkeb *et al.*, 2002; Janicka-Russak *et al.*, 2013). This would decrease the energy requirement for proton-mediated secondary active transport without increasing the inward gradient for passive Na^+ entry.

4. Is transmembrane Na^+ cycling a key determinant of cell energy use?

Excessive cycling of Na^+ and that of other ions in root cells of glycophytes is one of the most puzzling observations in plant transport physiology. Even if part of the tracer Na^+ uptake (and release in washout studies) reflected exchange with binding sites in the root apoplast (see above discussion in *Energetics of Na^+ transport: a conundrum*), there is evidence that a considerable fraction of Na^+ is indeed taken up by root cortical cells and is subsequently released again, either at the same cell or further up the root after the Na^+ is withdrawn from the xylem (Davenport *et al.*, 2005). The energetic costs of this cycling, if confirmed, calls for an investigation into the benefit the plant could potentially draw from such a process. It remains an intellectual challenge to understand why transport proteins allowing Na^+ entry into the root symplast exist in the plasma membrane, when salt exclusion is an important strategy to avoid saline stress in glycophytes. Earlier studies showed that salt-starved roots ('low salt roots') readily take up Na^+ to generate turgor when there is essentially no other choice (Pitman *et al.*, 1968), and obviously transport proteins are needed for this contingency. Because cells can express and alter their transporters to suit the conditions, the existence of a transport pathway for Na^+ entry does not mean that it is always operating. A contender for the NSCC, the aquaporin PIP2;1, is rapidly removed from the plasma membrane upon a salinity stress (Boursiac *et al.*, 2008), perhaps because of its ability to transport Na^+. However, this unavoidably compromises water transport and potentially K^+ transport, because PIP2;1 also can transport K^+ which is strongly linked in a broader sense to generation of turgor in plant cells .

It has been proposed that Na^+ influx via aquaporins may provide the driving force for simultaneous water uptake, via the same transport protein, against the water potential gradient (which may

favour water *efflux* instead). This would require a close coupling of water and solute transport, allowing a transfer of free energy between the fluxes, which can be tested experimentally. Nonosmotic water transport may play a role in the generation of root pressure, repair of embolized xylem vessels and control of cell elongation (Fricke, 2015; Wegner, 2015, 2017). This mechanism implies large circular fluxes of the solute(s) driving the water transport, because solutes permeating together with a fixed number of water molecules need to be re-translocated back immediately at the expense of metabolic energy to maintain the (electro)chemical gradient. This implies that the seemingly futile cycling of Na^+ and K^+ has a physiological function rather than being just a waste of energy. Evidence in support of this hypothesis has been provided previously (Wegner, 2017). It should be noted that the osmotic and nonosmotic water uptake mechanisms proposed by Wegner (2017) are mutually exclusive, at least at the cellular level, because water fluxes across the plasma membrane are facilitated by a high activity of aquaporins, which would short-circuit nonosmotic water uptake, rendering it unfeasible from an energetic point of view (Wegner, 2015, 2017; Fricke, 2017). These considerations may help to understand the complex regulation of aquaporin activity under salt stress (McGaughey *et al.*, 2018).

IV. Root anatomy and transport pathways

Pathways through root systems impact on the energy needed for plant salt tolerance. Plants must exclude nearly all the salt in the soil solution while taking up water, and maintain a low net rate of Na^+ and Cl^- uptake (Munns *et al.*, 2020). Here we assess three aspects that affect the ability of roots to exclude salt while taking up water, without exhausting the energy budget of the plant.

1. Root systems and the anatomies of root types

The most important aspect of roots compared to shoots is that the stele tissues (xylem, phloem, pericycle and parenchyma cells) are internal, surrounded by a cortex (the innermost layer of which is known as the endodermis) and an epidermis (Fig. 6a–d). Epidermal cells may differentiate into root hairs (Fig. 6e). Shoots have stele tissues distributed throughout parenchyma cells. Evidence has emerged that the root cortex must do the heavy lifting of excluding Na^+ from shoots (Munns *et al.*, 2020). Within this context, the large differences between cortex and stele anatomies are intriguing (Varney *et al.*, 1991; Watt *et al.*, 2008, 2009). Large variation depends on root type (axile versus branch types), age and soil (Fig. 6a–d).

The single root model underlies our current framework for salinity tolerance mechanisms (e.g. Fig. 5). This is generally an axile root from the embryo (seminal; Fig. 6a) or stem (nodal; Fig. 6d); branch roots are rarely considered (e.g. Faiyue *et al.*, 2012). The single root model greatly underestimates pathways for salts and water from soil to shoot, based on distances and cell sizes. In wheat, within 10 d of germination, the plant develops a system of different root types with branch roots (termed lateral or fine roots) that have emerged from an axile root (Fig. 6a or d). The complexity of the system increases with time: by the time of flowering, wheat roots below the topsoil can be 90% branch roots with the fine structure and anatomy shown in Fig. 6(c) (Watt *et al.*, 2008).

Soil conditions, including high salinity, strongly influence allocation between axile and branch roots (Rich & Watt, 2013). Durum wheat root systems were studied in a gradient of salinity, to mimic distribution under natural soil conditions (Rahnama *et al.*, 2011). Seminal axile root lengths in saline gradients were *c.* 25% *less* than those of the control, whereas branch length was *c.* 500% *greater*. The consequences of shifts to different root types could be large in terms of anatomy: in the saline gradient, *c.* 26% of total root length shifted to finer branch roots (e.g. Fig. 6b,c), and the branch roots emerged much closer to the axile tip (*c.* 3 cm in saline conditions compared with *c.* 20 cm in nonsaline).

Salinity inhibits cell division in the primary roots of species including wheat and barley (Rahnama *et al.* 2011; Shelden *et al.*, 2013). Branch root initiation and extension was uninhibited by external salt (Rahnama *et al.* 2011). Decreasing primary root length and allocating energy to the initiation of lateral roots may be linked to adaptation to salinity, a mechanism which also was seen by Zolla *et al.* (2010) in Arabidopsis. Branch roots arise from pericycle cells and water for elongation may come from the phloem (Boyer *et al.*, 2010). Salinity can promote differentiation of underlying xylem tissues in cotton (Reinhardt & Rost, 1995) and aging of roots in tomato (Snapp & Shennan, 1992). Taken together, these studies suggest that anatomical pathways across a root system may change upon exposure to saline soil compared to nonsaline conditions (Fig. 6f).

2. Importance of root system anatomical differences: estimating ATP costs of cortical cell layers

What could be the energy consequences of changing root anatomy on Na^+ transport costs? Here we compare scenarios of roots with single or double cortical cell layers to predict if root types may have different energy costs for Na^+, K^+ and Cl^- transport. An Arabidopsis model (Foster & Miklavcic, 2017) was applied to the simplest branch roots of wheat (Fig. 6c). Wheat fine roots share similarities with Arabidopsis roots (image in Fig. 6c inset), except that the wheat root tested had two cortical cell layers, whereas the Arabidopsis root had one.

The modelling predicts that a higher cortical cell layer number is associated with increased energy requirements for ion transport in salt-stressed roots (Fig. 6g). A modelled wheat root with only one cortical layer would use 20% less energy (per unit of root length) for ion transport than a root with two cortical cell layers. The plasma membrane surface area of the cells outside the endodermal apoplastic barrier correlate reasonably with the energy cost (Fig. 6h). The number of cells outside the outermost apoplastic barrier correlate with the energy cost better than the total root perimeter (or surface area).

The model used here presents one consequence of root system architecture differences under saline conditions (Fig. 6f). Anatomical changes to the root system to cope with salinity may lower the energy cost of ion movements across membranes that require ATP. The importance of living cell number to root energetics has been

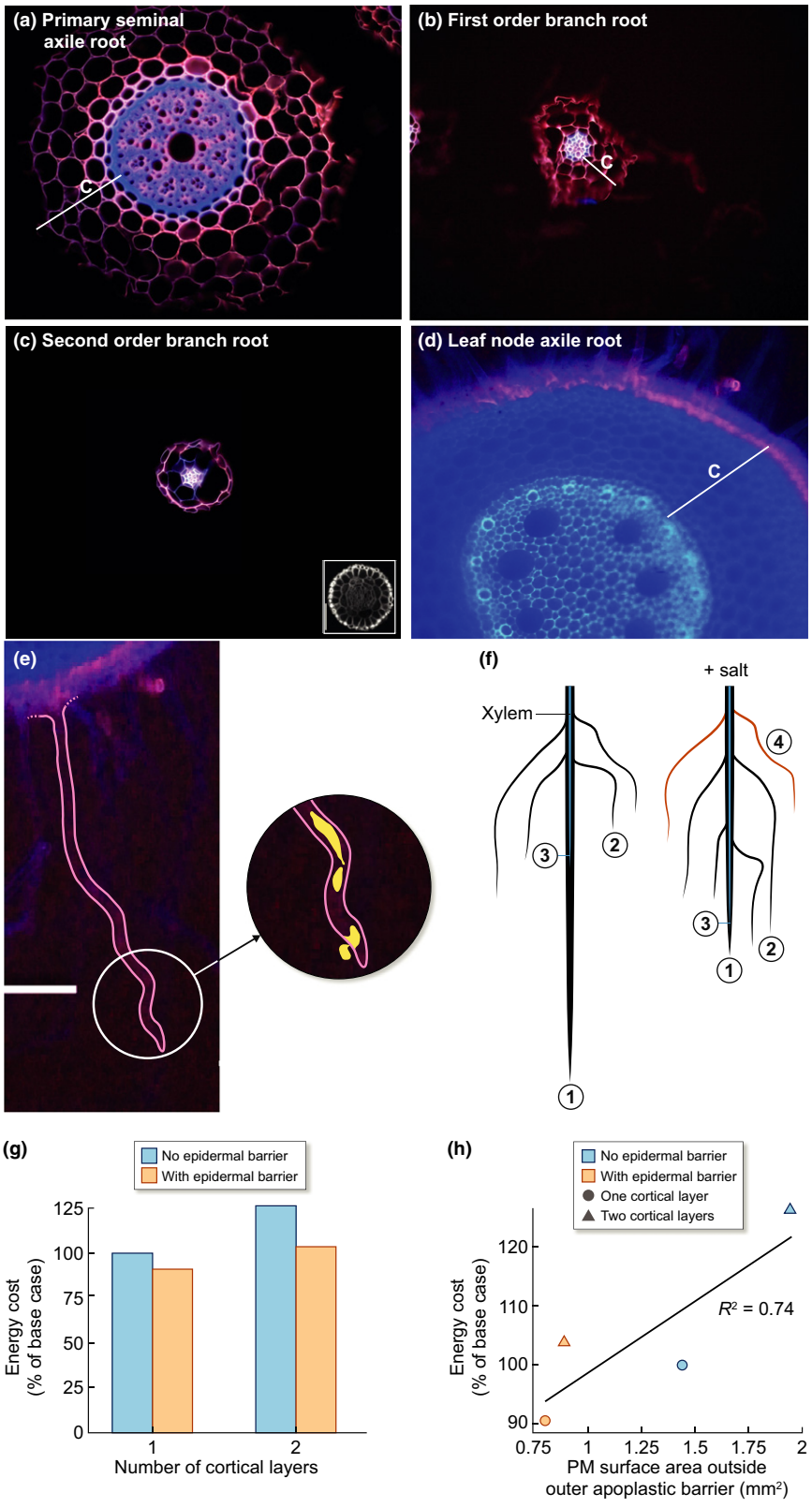

Fig. 6 Changes in anatomy, root system and root cells that may be important in the energetics of salinity tolerance. (a–d) Cross-sections of wheat roots, all at the same magnification. Inset of (c), Arabidopsis primary root cross-section, shown at same magnification as wheat second-order branch root (bar, 50 μm; from Sotta & Fujiwara, 2017). (e) Speculation about importance of root hairs as an epidermal barrier to Na^+ movement into the root. Left. Root hair of nodal root in (d) outlined to indicate surface area with soil. Right, enlargement of hair tip with hypothesized, drawn transport of vesicles (yellow) delivering Na^+ to the outside of the cells (bar, 25 μm). Speculation and drawing based on the root hairs of sorghum, which can transport sorgoleone to the surface and to the soil in vesicles (see the subsection 'Cell specializations at the epidermis including hair growth and functions'). (f) Schematic view of influence of salinity on a root system. Events: (1) shortening of primary root; (2) increased first-order branch root length; (3) branch root and xylem maturity closer to the tip; (4) increased rate of root aging. See text for references to original research for these events. (g) Modelled effects of either one or two cortical cell layers, and presence of an epidermal barrier, on energy costs of transmembrane transport. (h) Positive relationship between plasma membrane surface area outside an apoplastic barrier and energy cost. The Foster & Miklavcic (2017) model root geometry was adapted to simulate wheat roots with one or two cortical layers. For all simulations, the external medium contained 100 mM NaCl, and a hydraulic pressure of −0.3 MPa was assumed at the top boundary of the root. The remaining simulation conditions were as described in Foster & Miklavcic (2017) for the nonuniform transport scenario. C, cortex; PM, plasma membrane.

shown by Lynch and colleagues using modelling and measurements on plants exposed to low nutrient supply (e.g. Schneider *et al.*, 2017). Here we simulated fewer and smaller living cortical cells, not cortical cell senescence. Future studies are needed to test salinity stress tolerance implications of fewer cells with greater apoplasmic spaces.

3. Cell specializations at the epidermis including hair growth and functions

The energy costs of the cell-to-cell pathway (plasma membrane and tonoplast transport of Na^+, K^+ and Cl^-) could be high, especially in a nodal axile root with 11 cortical cell layers and a seminal axile root with six layers (cf. Fig. 6d with a). This prompts consideration of other possible mechanisms by which roots could prevent Na^+ from reaching shoots.

The plasma membrane of epidermal cells contains Na^+ transporters such as HvHKT1;1 in barley (Han *et al.*, 2018), and SOS1 in Arabidopsis (Shi *et al.*, 2002). This suggests that epidermal cells sense and have a role in excluding salt from the roots. Confocal microscopy was used to monitor the distribution of Na^+ using an indicator dye, and fluorescence was higher in the vacuole of the salt-tolerant variety, a finding that was supported by a much lower cytosolic to vacuole ratio of Na^+ (Cuin *et al.*, 2011; Wu *et al.*, 2018a,b). We estimated the effect of an apoplastic barrier in the epidermis on costs of ion transport in salt-stressed roots (Fig. 6g). An apoplastic epidermal barrier reduced the energy costs by 18% and 10% for the two and one cortical cell layer roots, respectively. These results indicate that an epidermal barrier could lead to larger energy savings in roots with more cortical layers.

Root hairs (Fig. 6e) have a larger surface-to-volume ratio than cortical cells and may capture most of the salt convected with water, retaining more salt from the soil solution than underlying cortical cells. Root hairs facilitate water uptake from soil at high transpiration rates (Carminati *et al.*, 2017). Root hairs were *c.* 50% shorter in response to salinity in barley, which is typical of studies conducted with seedlings in hydroponics without soil (see Shabala *et al.*, 2003). Root hair cells can develop specializations (Tyerman *et al.*, 1989), similar to modified trichomes on the aerial tissue of halophytes, known as epidermal bladder cells (EBC). EBC cells accumulate Na^+ in excess of that measured in mesophyll cells (Adams *et al.*, 1998; Barkla *et al.*, 2002). Interestingly, root hairs of the grass sorghum sequester compounds toxic to the cytoplasm in vacuoles and release them to soil by vesicular transport (Weston *et al.*, 2012). We speculate that root hairs may package salt into vesicles that are moved to the surface and extruded to the soil (Fig. 6e). Future studies of root hair responses and mechanisms of sequestering salt should be tested in soil and on different root types (Nestler *et al.*, 2016).

4. Membrane dynamics avoid transmembrane crossings

Traditionally, the cellular view is static, with cells requiring mechanisms to keep salt out of the cell or sequester into the vacuole. Improved imaging techniques in recent years show constant, highly dynamic construction and de-construction of membranes in contact with the apoplast (walls). The vacuole appears as a flexible bubble, widening and narrowing the space between the tonoplast and plasma membrane (Löfke *et al.*, 2015). This provides the opportunity for direct contact of the two membranes and the possibility of a direct 'shunt' for ions to enter the vacuole either without crossing through the cytosol or crossing via a cytosolic micro domain with different conditions (Flowers *et al.*, 2018).

Such membrane contact sites have been identified between other organelles within a distance of 10–30 nm (Wu *et al.*, 2018a,b). Evidence for direct channelling of ions between the endoplasmic reticulum (ER) and plasma membrane, and between ER and mitochondria (Prinz, 2014), opens the possibility for Na^+ ions to be transported in this manner. Once in the organellar lumen, the ions can be trafficked to the vacuole from the ER or pass through the Golgi and *trans*-Golgi network (TGN) to pre-vacuolar compartments and finally to the vacuole (Honscher *et al.*, 2014). These routes exclude the energetically costly cytosolic import and export steps. The ER of two cells is usually connected through the plasmodesmata (Thomas *et al.*, 2008), providing an avenue for ion movement between cells in the lumen without transport across membranes, followed by sequestration in the vacuole. We speculate that the energy costs of this movement could be lower than crossing vacuolar and plasma membranes (four crossings per cell).

In summary, root systems display multiple and flexible options to adjust the energetics of salinity tolerance using anatomy and cell differentiations. An additional option to Fig. 4 is multiple pathways with different modes of transport (and energetics) in space and time within a plant.

V. Where to from here?

Which of the many transport processes consume the most energy, and at what time and where in the plant? These questions are difficult to answer by experimental study alone. However, achieving a detailed, quantitative understanding of this complex whole-plant salt stress response is possible if physiological studies are accompanied by computational/biophysical modelling (Foster & Miklavcic, 2017). Biophysical models could be adapted to incorporate energy fluxes and used to identify transporters that may be engineered to achieve improved energy efficiency in roots. The effect of endodermal barriers on ion uptake and energy costs of ion transport through the root has been quantified by models (Foster & Miklavcic, 2016, 2017). Models of salt and water transport in a single plant cell (Foster & Miklavcic, 2015), and OnGuard software which models guard cell transport, homeostasis and metabolism (Chen *et al.*, 2012; Hills *et al.*, 2012; Wang *et al.*, 2017), could be adapted to calculate the energetic costs of salt tolerance. For example, analogous biophysical modelling would not only inform us of the transport mechanisms with the highest energy demands, but also allow us to identify transport steps as targets to minimize these energy costs while still maintaining conditions compatible with salt tolerance. In addition, biophysical modelling has the potential to answer questions on the quantity of ATP available. For example, existing models of transport in isolated plant cells combined with models of ATP production in animal cells (e.g. Bertram *et al.*, 2006) could be adapted to quantitatively model ATP production in plant mitochondria. Modelling also can be used to investigate currently unproven hypotheses, such as the possibility of water co-transport with ions such as Na^+ (Wegner, 2017). Although existing models of ion and water transport in plants assume that water transport is passive, they could be adapted to explore the possibility of active water transport.

A potentially important component to include in models of energy use is the signalling that occurs in response to salt stress, including involvement of transporters, that leads to changes in gene expression, growth and remodelling of root systems (Julkowska & Testerink, 2015), which ultimately affects the energetics. Another aspect not dealt with here is the costs of altering the proteome because protein synthesis can consume a large amount of energy; in leaves it could consume 25% of the ATP produced by respiration (L. Li *et al.*, 2017). Collaboration between theoreticians and experimentalists is needed to answer the questions raised here. This may address many of the gaps in our knowledge of salt tolerance mechanisms in plants. Accurate estimation of energy costs associated with salinity tolerance may provide a new approach to long-standing problems – by the coordinated measurements of transport activities and root respiration on the same tissue under the same conditions. This, together with identification of the molecular components in crop species that can be modified to increase the amount of energy available for harvestable yield (Amthor *et al.*, 2019), may provide a new approach to increase yield on saline soils.

Acknowledgements

This review was instigated from the 22nd New Phytologist Workshop 'Energy costs of salinity tolerance in crop plants' Adelaide, Australia, 10–12 April 2018 and we thank all participants for their contributions and discussion. RM, SDT, MG, CSB, JB, NLT, MS and SW acknowledge the financial assistance from The Australian Research Council Centre of Excellence in Plant Energy Biology (CE140100008).

ORCID

Borjana Arsova https://orcid.org/0000-0002-0566-2009
Bronwyn J. Barkla https://orcid.org/0000-0002-4691-8023
Jayakumar Bose https://orcid.org/0000-0002-0565-2951
Caitlin S. Byrt https://orcid.org/0000-0001-8549-2873
Zhong-Hua Chen https://orcid.org/0000-0002-7531-320X
David A. Day https://orcid.org/0000-0001-7967-2173
Kylie J. Foster https://orcid.org/0000-0003-2651-3915
Wieland Fricke https://orcid.org/0000-0002-1514-1389
Matthew Gilliham https://orcid.org/0000-0003-0666-3078
Sam W. Henderson https://orcid.org/0000-0003-3019-1891
Colin L. D. Jenkins https://orcid.org/0000-0002-9347-8948
Herbert J. Kronzucker https://orcid.org/0000-0002-9358-0029
Stanley J. Miklavcic https://orcid.org/0000-0002-2361-246X
Rana Munns https://orcid.org/0000-0002-7519-2698
Darren Plett https://orcid.org/0000-0002-9551-8755
Stuart J. Roy https://orcid.org/0000-0003-0411-9431
Sergey Shabala https://orcid.org/0000-0003-2345-8981
Megan C. Shelden https://orcid.org/0000-0002-7203-3763
Kathleen L. Soole https://orcid.org/0000-0002-8837-3404
Nicolas L. Taylor https://orcid.org/0000-0003-2004-5217
Mark Tester https://orcid.org/0000-0002-5085-8801
Stephen D. Tyerman https://orcid.org/0000-0003-2455-1643
Michelle Watt https://orcid.org/0000-0001-7843-0957
Stefanie Wege https://orcid.org/0000-0002-7232-5889
Lars H. Wegner https://orcid.org/0000-0002-9263-8436

References

Adams P, Nelson DE, Yamada S, Chmara W, Jensen RG, Bohnert HJ, Griffiths H. 1998. Growth and development of *Mesembryanthemum crystallinum* (Aizoaceae). *New Phytologist* **138**: 171–190.

Alexova R, Nelson CJ, Jacoby RP, Millar AH. 2015. Exposure of barley plants to low Pi leads to rapid changes in root respiration that correlate with specific alterations in amino acid substrates. *New Phytologist* **206**: 696–708.

Amthor JS. 2000. The McCree–de Wit–Penning de Vries–Thornley respiration paradigms: 30 years later. *Annals of Botany* **86**: 1–20.

Amthor JS, Bar-Even A, Hanson AD, Millar AH, Stitt M, Sweetlove LJ, Tyerman SD. 2019. Engineering strategies to boost crop productivity by cutting respiratory carbon loss. *Plant Cell* **31**: 297–314.

Asif MA, Schilling RK, Tilbrook J, Brien C, Dowling K, Rabie H, Short L, Trittermann C, Garcia A, Barrett-Lennard EG *et al.* 2018. Mapping of novel salt tolerance QTL in an Excalibur × Kukri doubled haploid wheat population. *Theoretical and Applied Genetics* **131**: 2179–2196.

Assmann SM, Zeiger E. 1987. Guard cell bioenergetics. In: Zeiger E, Farquhar GD, Cowan IR, eds. *Stomatal function*. Stanford, CA, USA: Stanford University Press, 163–193.

Barkla BJ, Vera-Estrella R, Camacho-Emiterio J, Pantoja O. 2002. Na^+/H^+ exchange in the halophyte *Mesembryanthemum crystallinum* is associated with cellular sites of Na^+ storage. *Functional Plant Biology* **29**: 1017–1024.

Bassil E, Tajima H, Liang YC, Ohto M, Ushijima K, Nakano R, Esumi T, Coku A, Belmonte M, Blumwald E. 2011. The Arabidopsis Na^+/H^+ antiporters NHX1 and NHX2 control vacuolar pH and K^+ homeostasis to regulate growth, flower development, and reproduction. *Plant Cell* **23**: 3482–3497.

Bassil E, Zhang S, Gong H, Tajima H, Blumwald E. 2019. Cation specificity of vacuolar NHX-type cation/H^+ antiporters. *Plant Physiology* **179**: 616–629.

Beauzamy L, Nakayama N, Boudaoud A. 2014. Flowers under pressure: ins and outs of turgor regulation in development. *Annals of Botany* **114**: 1517–1533.

Bertram R, Gram Pedersen M, Luciani DS, Sherman A. 2006. A simplified model for mitochondrial ATP production. *Journal of Theoretical Biology* **243**: 575–586.

Bijlsma RJ, Lambers H, Kooijman S. 2000. A dynamic whole-plant model of integrated metabolism of nitrogen and carbon. 1. Comparative ecological implications of ammonium-nitrate interactions. *Plant and Soil* **220**: 49–69.

Bloom AJ, Sukrapanna SS, Warner RL. 1992. Root respiration associated with ammonium and nitrate absorption and assimilation by barley. *Plant Physiology* **99**: 1294–1301.

Bonales-Alatorre E, Shabala S, Chen ZH, Pottosin I. 2013. Reduced tonoplast fast-activating and slow-activating channel activity is essential for conferring salinity tolerance in a facultative halophyte, Quinoa. *Plant Physiology* **162**: 940–952.

Bose J, Munns R, Shabala S, Gilliham M, Pogson B, Tyerman SD. 2017. Chloroplast function and ion regulation in plants growing on saline soils: lessons from halophytes. *Journal of Experimental Botany* **68**: 3129–3143.

Bose J, Rodrigo-Moreno A, Shabala S. 2014. ROS homeostasis in halophytes in the context of salinity stress tolerance. *Journal of Experimental Botany* **65**: 1241–1257.

Boursiac Y, Boudet J, Postaire O, Luu DT, Tournaire-Roux C, Maurel C. 2008. Stimulus-induced downregulation of root water transport involves reactive oxygen species-activated cell signalling and plasma membrane intrinsic protein internalization. *The Plant Journal* **56**: 207–218.

Boursiac Y, Chen S, Luu DT, Sorieul M, van den Dries N, Maurel C. 2005. Early effects of salinity on water transport in Arabidopsis roots. Molecular and cellular features of aquaporin expression. *Plant Physiology* **139**: 790–805.

Boyer JS, Silk WK, Watt M. 2010. Path of water for root growth. *Functional Plant Biology* **37**: 1105–1116.

Britto DT, Kronzucker HJ. 2006. Futile cycling at the plasma membrane: a hallmark of low-affinity nutrient transport. *Trends in Plant Science* **11**: 529–534.

Britto DT, Kronzucker HJ. 2009. Ussing's conundrum and the search for transport mechanisms in plants. *New Phytologist* **183**: 243–246.

Britto DT, Kronzucker HJ. 2015. Sodium efflux in plant roots: what do we really know? *Journal of Plant Physiology* **186–187**: 1–12.

Buch-Pedersen MJ, Rudashevskaya EL, Berner TS, Venema K, Palmgren MG. 2006. Potassium as an intrinsic uncoupler of the plasma membrane H^+-ATPase. *Journal of Biological Chemistry* **281**: 38285–38292.

Byrt CS, Zhao MC, Kourghi M, Bose J, Henderson SW, Qiu JE, Gilliham M, Schultz C, Schwarz M, Ramesh SA *et al.* 2017. Non-selective cation channel activity of aquaporin AtPIP2;1 regulated by Ca^{2+} and pH. *Plant, Cell & Environment* **40**: 802–815.

Carden DE, Diamond D, Miller AJ. 2001. An improved Na^+-selective microelectrode for intracellular measurements in plant cells. *Journal of Experimental Botany* **52**: 1353–1359.

Carden DE, Walker DJ, Flowers TJ, Miller AJ. 2003. Single-cell measurements of the contributions of cytosolic Na^+ and K^+ to salt tolerance. *Plant Physiology* **131**: 676–683.

Carillo P. 2018. GABA shunt in durum wheat. *Frontiers in Plant Science* **9**: 100.

Carminati A, Passioura JB, Zarebanadkouki M, Ahmed MA, Ryan PR, Watt M, Delhaize E. 2017. Root hairs enable high transpiration rates in drying soils. *New Phytologist* **216**: 771–781.

Chaumont F, Tyerman SD. 2014. Aquaporins: highly regulated channels controlling plant water relations. *Plant Physiology* **164**: 1600–1618.

Cheeseman JM. 1982. Pump-leak sodium fluxes in low salt corn roots. *The Journal of Membrane Biology* **70**: 157–164.

Cheeseman JM, Bloebaum PD, Wickens LK. 1985. Short term $^{22}Na^+$ and $^{42}K^+$ uptake in intact, mid-vegetative plants. *Physiologia Plantarum* **65**: 460–466.

Chen Z, Newman I, Zhou M, Mendham N, Zhang G, Shabala S. 2005. Screening plants for salt tolerance by measuring K^+ flux: a case study for barley. *Plant, Cell & Environment* **28**: 1230–1246.

Chen Z-H, Hills A, Bätz U, Amtmann A, Lew VL, Blatt MR. 2012. Systems dynamic modeling of the stomatal guard cell predicts emergent behaviors in transport, signaling, and volume control. *Plant Physiology* **159**: 1235–1251.

Che-Othman MH, Jacoby RP, Millar AH, Taylor NL. 2020. Wheat mitochondrial respiration shifts from the tricarboxylic acid cycle to the GABA shunt under salt stress. *New Phytologist* **225**: 1166–1180.

Che-Othman MH, Millar AH, Taylor NL. 2017. Connecting salt stress signalling pathways with salinity-induced changes in mitochondrial metabolic processes in C_3 plants. *Plant, Cell & Environment* **40**: 2875–2905.

Choi WG, Toyota M, Kim SH, Hilleary R, Gilroy S. 2014. Salt stress-induced Ca^{2+} waves are associated with rapid, long-distance root-to-shoot signaling in plants. *Proceedings of the National Academy of Sciences, USA* **111**: 6497–6502.

Colmenero-Flores JM, Martínez G, Gamba G, Vázquez N, Iglesias DJ, Brumós J, Talón M. 2007. Identification and functional characterization of cation–chloride cotransporters in plants. *The Plant Journal* **50**: 278–292.

Colmer TD, Epstein E, Dvorak J. 1995. Differential solute regulation in leaf blades of various ages in salt-sensitive wheat and a salt-tolerant wheat × *Lophopyrum elongatum* (Host) A. Love amphiploid. *Plant Physiology* **108**: 1715–1724.

Cubero-Font P, Maierhofer T, Jaslan J, Rosales Miguel A, Espartero J, Díaz-Rueda P, Müller Heike M, Hürter A-L, Al-Rasheid Khaled AS, Marten I *et al.* 2016. Silent S-type anion channel subunit SLAH1 gates SLAH3 open for chloride root-to-shoot translocation. *Current Biology* **26**: 2213–2220.

Cuin TA, Betts SA, Chalmandrier R, Shabala S. 2008. A root's ability to retain K^+ correlates with salt tolerance in wheat. *Journal of Experimental Botany* **59**: 2697–2706.

Cuin TA, Bose J, Stefano G, Deepa JHA, Tester M, Mancuso S, Shabala S. 2011. Assessing the role of root plasma membrane and tonoplast Na/H exchangers in salinity tolerance in wheat: *in planta* quantification results. *Plant, Cell & Environment* **34**: 947–961.

Cuin TA, Miller AJ, Laurie SA, Leigh RA. 2003. Potassium activities in cell compartments of salt-grown barley leaves. *Journal of Experimental Botany* **54**: 657–661.

Davenport R, James RA, Zakrisson-Plogander A, Tester M, Munns R. 2005. Control of sodium transport in durum wheat. *Plant Physiology* **137**: 807–818.

Davenport RJ, Muñoz-Mayor A, Jha D, Essah PA, Rus A, Tester M. 2007. The Na^+ transporter AtHKT1;1 controls retrieval of Na^+ from the xylem in Arabidopsis. *Plant, Cell & Environment* **30**: 497–507.

Davenport RJ, Tester M. 2000. A weakly voltage-dependent, nonselective cation channel mediates toxic sodium influx in wheat. *Plant Physiology* **122**: 823–834.

Delfine S, Alvino A, Villani MC, Loreto F. 1999. Restrictions to carbon dioxide conductance and photosynthesis in spinach leaves recovering from salt stress. *Plant Physiology* **119**: 1101–1106.

Del-Saz NF, Florez-Sarasa I, Clemente-Moreno MJ, Mhadhbi H, Flexas J, Fernie AR, Ribas-Carbó M. 2016. Salinity tolerance is related to cyanide-resistant alternative respiration in *Medicago truncatula* under sudden severe stress. *Plant, Cell & Environment* **39**: 2361–2369.

Del-Saz NF, Ribas-Carbo M, McDonald AE, Lambers H, Fernie AR, Florez-Sarasa I. 2017. An *in vivo* perspective of the role(s) of the alternative oxidase pathway. *Trends in Plant Science* **23**: 206–219.

Demidchik V, Maathuis FJM. 2007. Physiological roles of nonselective cation channels in plants: from salt stress to signalling and development. *New Phytologist* **175**: 387–404.

Demidchik V, Shabala S, Isayenkov S, Cuin TA, Pottosin I. 2018. Calcium transport across plant membranes: mechanisms and functions. *New Phytologist* **220**: 49–69.

Demidchik V, Tester M. 2002. Sodium fluxes through nonselective cation channels in the plasma membrane of protoplasts from Arabidopsis roots. *Plant Physiology* **128**: 379–387.

Dietz KJ, Schramm M, Lang B, Lanzl-Schramm A, Durr C, Martinoia E. 1992. Characterization of the epidermis from barley primary leaves: II. The role of the epidermis in ion compartmentation. *Planta* **187**: 431–437.

Faiyue B, Al-Azzawi MJ, Flowers TJ. 2012. A new screening technique for salinity resistance in rice (*Oryza sativa* L.) seedlings using bypass flow. *Plant, Cell & Environment* **35**: 1099–1108.

Felle HH. 1994. The H^+/Cl^- symporter in root-hair cells of *Sinapsis alba*. *Plant Physiology* **106**: 1131–1136.

Ferjani A, Segami S, Horiguchi G, Sakata A, Maeshima M, Tsukaya H. 2012. Regulation of pyrophosphate levels by H^+-PPase is central for proper resumption of early plant development. *Plant Signaling & Behavior* **7**: 38–42.

Flam-Shepherd R, Huynh WQ, Coskun D, Hamam AM, Britto DT, Kronzucker HJ. 2018. Membrane fluxes, bypass flows, and sodium stress in rice: the influence of silicon. *Journal of Experimental Botany* **69**: 1679–1692.

Flowers TJ, Glenn EP, Volkov V. 2018. Could vesicular transport of Na^+ and Cl^- be a feature of salt tolerance in halophytes? *Annals of Botany* **123**: 1–18.

Foster KJ, Miklavcic SJ. 2015. Toward a biophysical understanding of the salt stress response of individual plant cells. *Journal of Theoretical Biology* **385**: 130–142.

Foster KJ, Miklavcic SJ. 2016. Modeling root zone effects on preferred pathways for the passive transport of ions and water in plant roots. *Frontiers in Plant Science* **7**: 914.

Foster KJ, Miklavcic SJ. 2017. A comprehensive biophysical model of ion and water transport in plant roots. I. Clarifying the roles of endodermal barriers in the salt stress response. *Frontiers in Plant Science* **8**: 1326.

Fricke W. 2015. The significance of water co-transport for sustaining transpirational water flow in plants: a quantitative approach. *Journal of Experimental Botany* **66**: 731–739.

Fricke W. 2017. Water transport and energy. *Plant, Cell & Environment* **40**: 977–994.

Fricke W. 2020. Energy costs of salinity tolerance in crop plants: night-time transpiration and growth. *New Phytologist* **225**: 1152–1165.

Fricke W, Leigh RA, Tomos AD. 1994. Concentrations of inorganic and organic solutes in extracts from individual epidermal, mesophyll and bundle-sheath cells of barley leaves. *Planta* **192**:310–316.

Fricke W, Leigh RA, Tomos AD. 1996. The intercellular distribution of vacuolar solutes in the epidermis and mesophyll of barley leaves changes in response to NaCl. *Journal of Experimental Botany* **47**: 1413–1426.

Gaxiola RA, Regmi K, Paez-Valencia J, Pizzio G, Zhang S. 2016. Plant H^+-PPases: reversible enzymes with contrasting functions dependent on membrane environment. *Molecular Plant* **9**: 317–319.

Gilliham M, Dayod M, Hocking BJ, Xu B, Conn SJ, Kaiser BN, Leigh RA, Tyerman SD. 2011. Calcium delivery and storage in plant leaves: exploring the link with water flow. *Journal of Experimental Botany* **62**: 2233–2250.

Han Y, Yin SY, Huang L, Wu XL, Zeng JB, Liu XH, Qiu L, Munns R, Chen ZH, Zhang GP. 2018. A sodium transporter HvHKT1;1 confers salt tolerance in barley via regulating tissue and cell ion homeostasis. *Plant and Cell Physiology* **59**: 1976–1989.

He Y, Fu J, Yu C, Wang X, Jiang Q, Hong J, Lu K, Xue G, Yan C, James A. 2015. Increasing cyclic electron flow is related to Na^+ sequestration into vacuoles for salt tolerance in soybean. *Journal of Experimental Botany* **66**: 6877–6889.

Hedrich R, Mueller TD, Becker D, Marten I. 2018. Structure and function of TPC1 vacuole SV channel gains shape. *Molecular Plant* **11**: 764–775.

Henderson SW, Dunlevy JD, Wu Y, Blackmore DH, Walker RR, Edwards EJ, Gilliham M, Walker AR. 2018. Functional differences in transport properties of natural HKT1;1 variants influence shoot Na^+ exclusion in grapevine rootstocks. *New Phytologist* **217**: 1113–1127.

Hills A, Chen Z-H, Amtmann A, Blatt MR, Lew VL. 2012. OnGuard, a computational platform for quantitative kinetic modeling of guard cell physiology. *Plant Physiology* **159**: 1026–1042.

Honscher C, Mari M, Auffarth K, Bohnert M, Griffith J, Geerts W, van der Laan M, Cabrera M, Reggiori F, Ungermann C. 2014. Cellular metabolism regulates contact sites between vacuoles and mitochondria. *Developmental Cell* **30**: 86–94.

Husain S, von Caemmerer S, Munns R. 2004. Control of salt transport from roots to shoots of wheat in saline soil. *Functional Plant Biology* **31**: 1115–1126.

Isayenkov S, Isner JC, Maathuis FJM. 2010. Vacuolar ion channels: roles in plant nutrition and signalling. *FEBS Letters* **584**: 1982–1988.

Jacoby RP, Che-Othman MH, Millar AH, Taylor NL. 2016. Analysis of the sodium chloride-dependent respiratory kinetics of wheat mitochondria reveals differential effects on phosphorylating and non-phosphorylating electron transport pathways. *Plant, Cell & Environment* **39**: 823–833.

Jacoby RP, Millar AH, Taylor NL. 2013. Investigating the role of respiration in plant salinity tolerance by analyzing mitochondrial proteomes from wheat and a salinity-tolerant Amphiploid (wheat x *Lophopyrum elongatum*). *Journal of Proteome Research* **12**: 4807–4829.

Jacoby RP, Taylor NL, Millar AH. 2011. The role of mitochondrial respiration in salinity tolerance. *Trends in Plant Science* **16**: 614–623.

James RA, Rivelli AR, Munns R, von Caemmerer S. 2002. Factors affecting CO_2 assimilation, leaf injury and growth in salt-stressed durum wheat. *Functional Plant Biology* **29**: 1393–1403.

Janicka-Russak M, Kabala K, Wdowikowska A, Klobus G. 2013. Modification of plasma membrane proton pumps in cucumber roots as an adaptation mechanism to salt stress. *Journal of Plant Physiology* **170**: 915–922.

Julkowska MM, Testerink C. 2015. Tuning plant signaling and growth to survive salt. *Trends in Plant Science* **20**: 586–59.

Kerkeb L, Venema K, Donaire JP, Rodríguez-Rosales MP. 2002. Enhanced H^+/ATP coupling ratio of H^+-ATPase and increased 14-3-3 protein content in plasma membrane of tomato cells upon osmotic shock. *Physiologia Plantarum* **116**: 37–41.

Khadilkar AS, Yadav UP, Salazar C, Shulaev V, Paez-Valencia J, Pizzio GA, Gaxiola RA, Ayre BG. 2016. Constitutive and companion cell-specific overexpression of AVP1, encoding a proton-pumping pyrophosphatase, enhances biomass accumulation, phloem loading, and long-distance transport. *Plant Physiology* **170**: 401–414.

Kooijman S, Troost TA. 2007. Quantitative steps in the evolution of metabolic organisation as specified by the Dynamic Energy Budget theory. *Biological Reviews* **82**: 113–142.

Kourghi M, Nourmohammadi S, Pei JXV, Qiu JE, McGaughey S, Tyerman SD, Byrt CS, Yool AJ. 2017. Divalent cations regulate the ion conductance properties of diverse classes of aquaporins. *International Journal of Molecular Sciences* **18**: 19.

Kramer DM, Evans JR. 2011. The importance of energy balance in improving photosynthetic productivity. *Plant Physiology* **155**: 70–78.

Krasensky J, Jonak C. 2012. Drought, salt, and temperature stress-induced metabolic rearrangements and regulatory networks. *Journal of Experimental Botany* **63**: 1593–1608.

Kriegel A, Andrés Z, Medzihradszky A, Krüger F, Scholl S, Delang S, Patir-Nebioglu MG, Gute G, Yang H, Murphy AS *et al.* 2015. Job sharing in the endomembrane system: vacuolar acidification requires the combined activity of V-ATPase and V-PPase. *Plant Cell* **27**: 3383–3396.

Krishnamurthy P, Ranathunge K, Nayak S, Schreiber L, Mathew MK. 2011. Root apoplastic barriers block Na^+ transport to shoots in rice (*Oryza sativa* L.). *Journal of Experimental Botany* **62**: 4215–4228.

Kronzucker HJ, Britto DT. 2011. Sodium transport in plants: a critical review. *New Phytologist* **189**: 54–81.

Kurimoto K, Day DA, Lambers H, Noguchi K. 2004. Effect of respiratory homeostasis on plant growth in cultivars of wheat and rice. *Plant, Cell & Environment* **27**: 853–862.

Leigh R, Tomos A. 1993. Ion distribution in cereal leaves: pathways and mechanisms. *Philosophical Transactions of the Royal Society of London. Series B: Biological Sciences* **341**: 75–86.

Li B, Tester M, Gilliham M. 2017. Chloride on the move. *Trends in Plant Science* **22**: 236–248.

Li L, Nelson CJ, Trösch J, Castleden I, Huang S, Millar AH. 2017. Protein degradation rate in *Arabidopsis thaliana* leaf growth and development. *Plant Cell* **29**: 207–228.

Li WYF, Wong FL, Tsai SN, Phang TH, Shao GH, Lam HM. 2006. Tonoplast-located GmCLC1 and GmNHX1 from soybean enhance NaCl tolerance in transgenic bright yellow (BY)-2 cells. *Plant, Cell & Environment* **29**: 1122–1137.

Löfke C, Dünser K, Scheuring D, Kleine-Vehn J. 2015. Auxin regulates SNARE-dependent vacuolar morphology restricting cell size. *eLife* **4**: e05868.

Lorenzen I, Aberle T, Plieth C. 2004. Salt stress-induced chloride flux: a study using transgenic Arabidopsis expressing a fluorescent anion probe. *The Plant Journal* **38**: 539–544.

Malagoli P, Britto DT, Schulze LM, Kronzucker HJ. 2008. Futile Na^+ cycling at the root plasma membrane in rice (*Oryza sativa* L.): kinetics, energetics, and relationship to salinity tolerance. *Journal of Experimental Botany* **59**: 4109–4117.

Maurel C, Boursiac Y, Luu DT, Santoni V, Shahzad Z, Verdoucq L. 2015. Aquaporins in plants. *Physiological Reviews* **95**: 1321–1358.

McGaughey SA, Qiu J, Tyerman SD, Byrt CS. 2018. Regulating root aquaporin function in response to changes in salinity. *Annual Plant Reviews online*. doi: 10.1002/9781119312994.apr0626.

Millar AH, Atkin OK, Menz RI, Henry B, Farquhar G, Day DA. 1998. Analysis of respiratory chain regulation in roots of soybean seedlings. *Plant Physiology* **117**: 1083–1093.

Millar AH, Whelan J, Soole KL, Day DA. 2011. Organization and regulation of mitochondrial respiration in plants. *Annual Reviews of Plant Biology* **62**: 79–104.

Miller GAD, Suzuki N, Ciftci-Yilmaz S, Mittler RON. 2010. Reactive oxygen species homeostasis and signalling during drought and salinity stresses. *Plant, Cell & Environment* **33**: 453–467.

Munns R. 2002. Comparative physiology of salt and water stress. *Plant, Cell & Environment* **25**: 239–250.

Munns R, Gilliham M. 2015. Salinity tolerance of crops – what is the cost? *New Phytologist* **208**: 668–673.

Munns R, James RA, Xu B, Athman A, Conn SJ, Jordans C, Byrt CS, Hare RA, Tyerman SD, Tester M *et al.* 2012. Wheat grain yield on saline soils is improved by an ancestral Na^+ transporter gene. *Nature Biotechnology* **30**: 360–364.

Munns R, Passioura JB, Colmer TD, Byrt CS. 2020. Osmotic adjustment and energy limitations to plant growth in saline soil. *New Phytologist* **225**: 1091–1096.

Munns R, Tester M. 2008. Mechanisms of salinity tolerance. *Annual Review of Plant Biology* **59**: 651–681.

Nestler J, Keyes SD, Wissuwa M. 2016. Root hair formation in rice (*Oryza sativa* L.) differs between root types and is altered in artificial growth conditions. *Journal of Experimental Botany* **67**: 3699–3708.

Nguyen CT, Agorio A, Jossier M, Depre S, Thomine S, Filleur S. 2016. Characterization of the chloride channel-like, AtCLCg, involved in chloride tolerance in *Arabidopsis thaliana*. *Plant and Cell Physiology* **57**: 764–775.

Nunes-Nesi A, Araújo WL, Obata T, Fernie AR. 2013. Regulation of the mitochondrial tricarboxylic acid cycle. *Current Opinion in Plant Biology* **16**: 335–343.

Palmgren MG. 2001. Plant plasma membrane H^+-ATPases: powerhouses for nutrient uptake. *Annual Review of Plant Physiology and Plant Molecular Biology* **52**: 817–845.

Pedersen JT, Kanashova T, Dittmar G, Palmgren M. 2018. Isolation of native plasma membrane H^+-ATPase (Pma1p) in both the active and basal activation states. *FEBS Open Bio* **8**: 774–783.

Peng C, Uygun S, Shiu SH, Last RL. 2015. The impact of the branched-chain ketoacid dehydrogenase complex on amino acid homeostasis in Arabidopsis. *Plant Physiology* **169**: 1807–1820.

Percey WJ, McMinn A, Bose J, Breadmore MC, Guijt RM, Shabala S. 2016. Salinity effects on chloroplast photosystem II performance in glycophytes and halophytes. *Functional Plant Biology* **43**: 1003–1015.

Perez V, Wherrett T, Shabala S, Muniz J, Dobrovinskaya O, Pottosin I. 2008. Homeostatic control of slow vacuolar channels by luminal cations and evaluation of the channel-mediated tonoplast Ca^{2+} fluxes *in situ*. *Journal of Experimental Botany* **59**: 3845–3855.

Picco A, Mund M, Ries J, Nédélec F, Kaksonen M. 2015. Visualizing the functional architecture of the endocytic machinery. *eLife* **4**: e04535.

Pitman MG, Courtice AC, Lee B. 1968. Comparison of potassium and sodium uptake by barley roots at high and low salt status. *Australian Journal of Biological Sciences* **21**: 871–881.

Pizzio GA, Paez-Valencia J, Khadilkar AS, Regmi K, Patron-Soberano A, Zhang S, Sanchez-Lares J, Furstenau T, Li J, Sanchez-Gomez C *et al.* 2015. Arabidopsis type I proton-pumping pyrophosphatase expresses strongly in phloem, where it is required for pyrophosphate metabolism and photosynthate partitioning. *Plant Physiology* **167**: 1541–1553.

Pottosin I, Dobrovinskaya O. 2018. Two-pore cation (TPC) channel: not a shorthanded one. *Functional Plant Biology* **45**: 83–92.

Pottosin I, Schnknecht G. 2007. Vacuolar calcium channels. *Journal of Experimental Botany* **58**: 1559–1569.

Prinz WA. 2014. Bridging the gap: membrane contact sites in signaling, metabolism, and organelle dynamics. *Journal of Cell Biology* **205**: 759–769.

Rahnama A, Munns R, Poustini K, Watt M. 2011. A screening method to identify genetic variation in root growth response to a salinity gradient. *Journal of Experimental Botany* **62**: 69–77.

Qiu J, Henderson SW, Tester M, Roy SJ, Gilliham M. 2017. SLAH1, a homologue of the slow type anion channel SLAC1, modulates shoot Cl^- accumulation and salt tolerance in *Arabidopsis thaliana*. *Journal of Experimental Botany* **68**: 4495–4505.

Raven JA. 1985. Regulation of pH and generation of osmolarity in vascular plants – a cost-benefit analysis in relation to efficiency of use of energy, nitrogen and water. *New Phytologist* **101**: 25–77.

Rawson H. 1986. Gas exchange and growth in wheat and barley grown in salt. *Functional Plant Biology* **13**: 475–489.

Rawson HM, Gardner PA, Long MJ. 1987. Sources of variation in specific leaf-area in wheat grown at high-temperature. *Australian Journal of Plant Physiology* **14**: 287–298.

Reinhardt DH, Rost TL. 1995. On the correlation of primary root growth and tracheary element size and distance from the tip in cotton seedlings grown under salinity. *Environmental and Experimental Botany* **35**: 575–588.

Ribas-Carbo M, Taylor NL, Giles L, Busquets S, Finnegan PM, Day DA, Lambers H, Medrano H, Berry JA, Flexas J. 2005. Effects of water stress on respiration in soybean leaves. *Plant Physiology* **139**: 466–473.

Rich SM, Watt M. 2013. Soil conditions and cereal root system architecture: review and considerations for linking Darwin and Weaver. *Journal of Experimental Botany* **64**: 1193–1208.

Rivelli AR, James RA, Munns R, Condon AG. 2002. Effect of salinity on water relations and growth of wheat genotypes with contrasting sodium uptake. *Functional Plant Biology* **29**: 1065–1074.

Sade N, Galle A, Flexas J, Lerner S, Peleg G, Yaaran A, Moshelion M. 2014. Differential tissue-specific expression of NtAQP1 in *Arabidopsis thaliana* reveals a role for this protein in stomatal and mesophyll conductance of CO_2 under standard and salt-stress conditions. *Planta* **239**: 357–366.

Saleh L, Plieth C. 2013. A9C sensitive Cl^--accumulation in *A. thaliana* root cells during salt stress is controlled by internal and external calcium. *Plant Signaling & Behavior* **8**: e24259.

Scafaro AP, Negrini ACA, O'Leary B, Rashid FAA, Hayes L, Fan YZ, Zhang Y, Chochois V, Badger MR, Millar AH *et al.* 2017. The combination of gas-phase fluorophore technology and automation to enable high-throughput analysis of plant respiration. *Plant Methods* **13**: 13.

Scheurwater I, Dunnebacke M, Eising R, Lambers H. 2000. Respiratory costs and rate of protein turnover in the roots of a fast-growing (*Dactylis glomerata* L.) and a slow-growing (*Festuca ovina* L.) grass species. *Journal of Experimental Botany* **51**: 1089–1097.

Schilling RK, Tester M, Marschner P, Plett DC, Roy SJ. 2017. AVP1: one protein, many roles. *Trends in Plant Science* **22**: 154–162.

Schneider HM, Postma JA, Wojciechowski T, Kuppe C, Lynch JP. 2017. Root cortical senescence improves growth under suboptimal availability of N, P, and K. *Plant Physiology* **174**: 2333–2347.

Selinski J, Scheibe R, Day DA, Whelan JB. 2018. Alternative oxidase is positive for plant performance. *Trends in Plant Science* **23**: 588–597.

Shabala S, Shabala L, Barcelo J, Poschenrieder C. 2014. Membrane transporters mediating root signalling and adaptive responses to oxygen deprivation and soil flooding. *Plant, Cell & Environment* **37**: 2216–2233.

Shabala S, Chen G, Chen Z-H, Pottosin I. 2020. The energy cost of the tonoplast futile sodium leak. *New Phytologist* **225**: 1105–1110.

Shabala S, Shabala L, Van Volkenburgh E. 2003. Effect of calcium on root development and root ion fluxes in salinised barley seedlings. *Functional Plant Biology* **30**: 507–514.

Shatil-Cohen A, Attia Z, Moshelion M. 2011. Bundle-sheath cell regulation of xylem-mesophyll water transport via aquaporins under drought stress: a target of xylem-borne ABA? *The Plant Journal* **67**: 72–80.

Shelden MC, Roessner U, Sharp RE, Tester M, Bacic A. 2013. Genetic variation in the root growth response of barley genotypes to salinity stress. *Functional Plant Biology* **40**: 516–530.

Shi H, Lee B-H, Wu S-J, Zhu J-K. 2003. Overexpression of a plasma membrane Na^+/H^+ antiporter gene improves salt tolerance in *Arabidopsis thaliana*. *Nature Biotechnology* **21**: 81–85.

Shi HZ, Quintero FJ, Pardo JM, Zhu JK. 2002. The putative plasma membrane Na^+/H^+ antiporter SOS1 controls long-distance Na^+ transport in plants. *Plant Cell* **14**: 465–477.

Shi L-X, Theg SM. 2013. Energetic cost of protein import across the envelope membranes of chloroplasts. *Proceedings of the National Academy of Sciences, USA* **110**: 930–935.

Siedow JN, Day DA. 2000. Respiration and photorespiration. In: Buchanan BB, Gruissem W, Jones RL, eds. *Biochemistry and molecular biology of plants*. Rockville, MD, USA: American Society of Plant Physiologists, 676–728.

Skerrett M, Tyerman SD. 1994. A channel that allows inwardly directed fluxes of anions in protoplasts derived from wheat roots. *Planta* **192**: 295–305.

Smith CA, Melino VJ, Sweetman C, Soole KL. 2009. Manipulation of alternative oxidase can influence salt tolerance in *Arabidopsis thaliana*. *Physiologia Plantarum* **137**: 459–472.

Snapp SS, Shennan C. 1992. Effects of salinity on root growth and death dynamics of tomato, *Lycopersicon esculentum* Mill. *New Phytologist* **121**: 71–79.

Sotta N, Fujiwara T. 2017. Preparing thin cross sections of *Arabidopsis* roots without embedding. *BioTechniques* **63**: 281–283.

Teakle NL, Tyerman SD. 2010. Mechanisms of Cl^- transport contributing to salt tolerance. *Plant, Cell & Environment* **33**: 566–589.

Thomas CL, Bayer EM, Ritzenthaler C, Fernandez-Calvino L, Maule AJ. 2008. Specific targeting of a plasmodesmal protein affecting cell-to-cell communication. *PLoS Biology* **6**: e7.

Tyerman SD, Oats P, Gibbs J, Dracup M, Greenway H. 1989. Turgor-volume regulation and cellular water relations of *Nicotiana tabacum* roots grown in high salinities. *Australian Journal of Plant Physiology* **16**: 517–531.

Tyerman SD, Skerrett M, Garrill A, Findlay GP, Leigh RA. 1997. Pathways for the permeation of Na^+ and Cl^- into protoplasts derived from the cortex of wheat roots. *Journal of Experimental Botany* **48**: 459–480.

Ussing HH. 1947. Interpretation of the exchange of radio-sodium in isolated muscle. *Nature* **160**: 262.

Ussing HH. 1994. Does active transport exist? *The Journal of Membrane Biology* **137**: 91–98.

Van Den Boogaard R, Goubitz S, Veneklaas EJ, Lambers H. 1996. Carbon and nitrogen economy of four *Triticum aestivum* cultivars differing in relative growth rate and water use efficiency. *Plant, Cell & Environment* **19**: 998–1004.

Vanlerberghe GC. 2013. Alternative oxidase: a mitochondrial respiratory pathway to maintain metabolic and signaling homeostasis during abiotic and biotic stress in plants. *International Journal of Molecular Sciences* **14**: 6805–6847.

Varney GT, Canny MJ, Wang XL, McCully ME. 1991. The branch roots of *Zea*. I. First order branches, their number, sizes and division into classes. *Annals of Botany* **67**: 357–364.

Venema K, Palmgren MG. 1995. Metabolic modulation of transport coupling ratio in yeast plasma-membrane H^+-ATPase. *Journal of Biological Chemistry* **270**: 19659–19667.

Volkov V. 2015. Salinity tolerance in plants. Quantitative approach to ion transport starting from halophytes and stepping to genetic and protein engineering for manipulating ion fluxes. *Frontiers in Plant Science* **6**: 25.
Walker BJ, VanLoocke A, Bernacchi CJ, Ort DR. 2016. The costs of photorespiration to food production now and in the future. *Annual Review of Plant Biology* **67**: 107–129.
Wang S-M, Zhang J-L, Flowers TJ. 2007. Low-affinity Na^+ uptake in the halophyte *Suaeda maritima*. *Plant Physiology* **145**: 559–571.
Wang Y, Hills A, Vialet-Chabrand S, Papanatsiou M, Griffiths H, Rogers S, Lawson T, Lew VL, Blatt MR. 2017. Unexpected connections between humidity and ion transport discovered using a model to bridge guard cell-to-leaf scales. *Plant Cell* **29**: 2921–2939.
Watt M, Magee LJ, McCully ME. 2008. Types, structure and potential for axial water flow in the deepest roots of field-grown cereals. *New Phytologist* **178**: 135–146.
Watt M, Schneebeli K, Dong P, Wilson IW. 2009. The shoot and root growth of *Brachypodium* and its potential as a model for wheat and other cereal crops. *Functional Plant Biology* **36**: 960–969.
Wegner LH. 2015. A thermodynamic analysis of the feasibility of water secretion into xylem vessels against a water potential gradient. *Functional Plant Biology* **42**: 828–835.
Wegner LH. 2017. Cotransport of water and solutes in plant membranes: the molecular basis, and physiological functions. *Aims Biophysics* **4**: 192–209.
Wen Z, Tyerman S, Dechorgnat J, Ovchinnikova E, Dhugga K, Kaiser BN. 2017. Maize NPF6 proteins are homologs of Arabidopsis CHL1 that are selective for both nitrate and chloride. *Plant Cell* **29**: 2581–2596.
Weston LA, Ryan PR, Watt M. 2012. Mechanisms for cellular transport and release of allelochemicals from plant roots into the rhizosphere. *Journal of Experimental Botany* **63**: 3445–3454.
Wingler A, Lea PJ, Quick WP, Leegood RC. 2000. Photorespiration: metabolic pathways and their role in stress protection. *Philosophical Transactions of the Royal Society of London. Series B: Biological Sciences* **355**: 1517–1529.
Wu H, Carvalho P, Voeltz GK. 2018a. Here, there, and everywhere: the importance of ER membrane contact sites. *Science* **361**: 640.
Wu HH, Shabala L, Azzarello E, Huang YQ, Pandolfi C, Su NN, Wu Q, Cai SG, Bazihizina N, Wang L *et al.* 2018b. Na^+ extrusion from the cytosol and tissue-specific Na^+ sequestration in roots confer differential salt stress tolerance between durum and bread wheat. *Journal of Experimental Botany* **69**: 3987–4001.
Wu HH, Shabala L, Liu XH, Azzarello E, Zhou M, Pandolfi C, Chen ZH, Bose J, Mancuso S, Shabala S. 2015. Linking salinity stress tolerance tissue-specific Na^+ sequestration in wheat roots. *Frontiers in Plant Science* **6**: 13.
Xu B, Hrmova M, Gilliham M. 2019. High affinity Na^+ transport by wheat HKT1;5 is blocked by K^+. *BioRxiv*. doi: 10.1101/280453.
Yeo AR, Yeo ME, Flowers TJ. 1987. The Contribution of an apoplastic pathway to sodium uptake by rice roots in saline conditions. *Journal of Experimental Botany* **38**: 1141–1153.
Zhu M, Zhou M, Shabala L, Shabala S. 2017. Physiological and molecular mechanisms mediating xylem Na^+ loading in barley in the context of salinity stress tolerance. *Plant, Cell & Environment* **40**: 1009–1020.
Zolla G, Heimer YM, Barak S. 2010. Mild salinity stimulates a stress-induced morphogenic response in *Arabidopsis thaliana* roots. *Journal of Experimental Botany* **61**: 211–224.

Supporting Information

Additional Supporting Information may be found online in the Supporting Information section at the end of the article.

Notes S1 Net stoichiometry and ATP yield of sucrose oxidation with and without alternative oxidase, and energy budget for photosynthesis.

Please note: Wiley Blackwell are not responsible for the content or functionality of any Supporting Information supplied by the authors. Any queries (other than missing material) should be directed to the *New Phytologist* Central Office.

See also the Commentary on this article by Sanders, **225**: 1047–1048.